Fuel 344 (2023) 128102

Contents lists available at ScienceDirect

Fuel

journal homepage: www.elsevier.com/locate/fuel

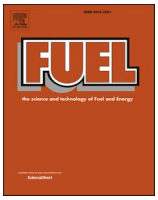

Current status of CO_2 capture with ionic liquids: Development and progress

Wamda Faisal Elmobarak [a], Fares Almomani [a,*], Muhammad Tawalbeh [b,c], Amani Al-Othman [d], Remston Martis [d], Kashif Rasool [e]

[a] Department of Chemical Engineering, Qatar University, P. O. Box 2713, Doha, Qatar
[b] Department of Sustainable and Renewable Energy Engineering, University of Sharjah, Sharjah P.O. Box 27272, United Arab Emirates
[c] Sustainable Energy & Power Systems Research Centre, RISE, University of Sharjah, P.O. Box 27272, Sharjah, United Arab Emirates
[d] Department of Chemical and Biological Engineering, American University of Sharjah, Sharjah, P.O. Box 26666, United Arab Emirates
[e] Qatar Environment and Energy Research Institute (QEERI), Hamad Bin Khalifa University, Qatar Foundation, P.O. Box 5825, Doha, Qatar

ARTICLE INFO

Keywords:
Biodegradability
CO_2 capture (CAP_{CO_2})
CO_2 uptake (UP_{CO_2}) capacity
Toxicity

ABSTRACT

Global warming triggered by greenhouse gas (GHG) emissions, particularly carbon dioxide (CO2), significantly influences climate change and has become a common environmental issue recently. The current amine-based technologies (ABTs) for CO_2 capture (CAP_{CO_2}) have high energy demand, low absorption, and desorption rates, and are less environmentally sustainable due to high emissions of volatile solvents. Therefore, the development of environmentally friendly CAP_{CO_2} materials and/or processes is a growing area of research. The utilization of ionic liquids (ILs) for CAP_{CO_2} has recently attracted attention. The unique characteristics of ILs, such as their low vapor pressure and high affinity for CAP_{CO_2} as well as their low volatility make them a viable substitute for the existing processes. This work provides a comprehensive overview of the accomplishments and challenges during the use of ILs for CAP_{CO_2}. The Review also outlines the mechanisms of the CAP_{CO_2} with ILs at the molecular level, the properties of ILs, characterization of the CO_2/IL systems, and the effect of operating conditions on CO_2 uptake (UP_{CO_2}) capacity by ILs. It also emphasizes the impact of cations, anions, and functional groups on the solubility of CO_2 ((S_{CO_2})) in ILs as well as the biodegradability and toxicity of ILs. Additionally, recent advances in IL membrane technology for the CAP_{CO_2} processes are considered. Lastly, the contribution of molecular simulations to create and assess ILs was reviewed. Protic and aprotic ILs properties have shown outstanding efficiency of UP_{CO_2}. The interactions between the anionic part of IL and CO_2 enhance the UP_{CO_2} and outperform the efficiency of traditional organic solvents. Functionalized ionic liquids (FUN_{ILs}) with tuned functional groups, supported ionic liquids membranes (SILMs) as well as reversible ionic liquids (RILs) have improved the efficiency of ILs as a promising CO_2 capturing process from industrial streams even under low CO_2 partial pressure. The relative importance of the chemical breakdown of the IL constituents (cation–anion interfacial structuring) during the CAP_{CO_2} process at different operating temperatures is unclear, and more research in this area is required to better inform the design of new ILs. This review provides a proper/systematic guideline to help ILs manufacturers and engineers design high-capacity ILs for appropriate CAP_{CO_2}.

1. Introduction

Since the industrial revolution, there has been a steady increase in CO_2 emissions into the environment, creating a global climate dilemma of how to reduce such greenhouse gas (GHG) emissions [1,2,313]. The CO_2 levels have risen from nearly 280 ppm around the time of the industrial revolution to 390 ppm today [3,314]. Global CO_2 emissions were reported to be 29.4 gigatonnes (Gt) in the last decade, representing a 50% increase from 20.9 Gt in 1990 [4]. The energy sector accounts for 41% of total energy associated with CO_2 emissions, while the transportation, industrial, and building sectors account for 23%, 20%, and 10%, respectively [5]. Burning fossil fuels to generate heat and power is the primary cause of the energy sector's high CO_2 emissions [6,7]. Using coal fuel produces 43% of CO_2 emissions, compared to oil's 37% and gas's 20%, respectively. [8]. With the increase in energy demand, CO_2 emissions are expected to increase two-fold per year to reach 28.8 Gt in 2050 [9]. With such a scenario, GHG emissions will continue making it impossible to maintain the global mean temperature within 2 °C above the pre-industrial level [10,11]. As a result, it appears that efficient

* Corresponding author.
E-mail address: falmomani@qu.edu.qa (F. Almomani).

https://doi.org/10.1016/j.fuel.2023.128102
Received 5 January 2023; Received in revised form 28 February 2023; Accepted 7 March 2023
Available online 15 March 2023

Nomenclature

GHG	Greenhouse gas
ABTs	Amine-based technologies
CAP_{CO_2}	CO_2 capture
S_{CO_2}	Solubility of CO_2
CCUS	Carbon capture, utilization, and storage
MEA	Monoethanolamine
MOFs	Metal-organic frameworks
ILs	Ionic liquids
IBILs	Imidazolium based ILs
$Post_{com}$	Post-combustion
Pre_{com}	Precombustion
Oxy_{com}	Oxyfuel combustion
SEL_{CO_2}	Selectivity to of CO_2
V_{IL}	Viscosity of IL
DGA	Diglycolamine
DEA	dDiethanolamine
DIPA	Diisopropylamine
MDEA	Methyl diethanolamine
TEA	Triethanolamine
WGS	Water-gas-shift
PILs	Protic ionic liquids
AILs	Aprotic ionic liquids
VIS_{CO_2}	Viscosity
VOL_{CO_2}	Volatility
UP_{CO_2}	Up take of CO_2
$[P_{666,14}]$	Phosphonium cation
IL_{FV}	Free volume of ILs
$[Tf_2N]$	Bis(trifluoromethyl sulfonyl)amide
IL_{VDMV}	Van der Waals molar volume
H_c	Henry coefficient
IL_{MFV}	Molar free volume of ILs
MW_{ILs}	Ionic Liquid molecular weight
$[bmim][PF_6]$	1-hexyl-3-methylimidazolium hexafluorophosphate
$[hmim][Tf_2N]$	1-hexyl-3-methylimidazolium trifluoromethanesulfonate
$[N_{4111}]$	N-butyl-N,N,N-trimethylammonium
$[bmim][MeSO_4]$	1-butyl-3-methylimidazolium methylsulfate
$[bmim][BF_4]$	1-butyl-3-methylimidazolium tetrafluoroborate
[omim]	1-octyl-3-methyl imidazolium
[hmim]	Imidazolium
[hmpy]	Pyridinium
[hmpyrr]	Pyrrolidinium
$[P_{2228}]$	Phosphonium
$[N_{2228}]$	Ammonium
D	Diffusion coefficients
ΔH_{vap}	Enthalpy of vaporization
Tb	Boiling temperature
VLE	Liquid-vapor equilibrium
FUN_{ILs}	Functionalized ionic liquids
$CAT\text{-}FUN_{ILs}$	Cationic-functionalized ILs
$AN\text{-}FUN_{ILs}$	Anionic-functionalized ILs
$CAT/AN\text{-}FUN_{ILs}$	Dual-functionalized ILs
IL_{poly}	Imidazolium-based poly ILs
NRTIL	Nongrafted room-temperature ionic liquid
$AN\text{-}FUN_{ILS}$	Anionic Functionalization ILs
$[P_{666,14}][Met]$	Trihexyl(tetradecyl)phosphonium methionate
$[P_{66614}][Pro]$	trihexyl(tetradecyl)phosphonium prolinate
$[P_{66614}]$	Trihexyl(tetradecyl)-phosphonium
$[bpy][BF_4]$	1-Butylpyridinium
[hmim]	1-n-hexyl-3-methylimidazolium
$[omim][BF_4]$	1-methyl-3-octylimidazolium tetrafluoroborate
[APMIM][Lys]	1-aminopropyl-3-methylimidazolium lysine
[N1111][Gly	Tetramethylammonium glycinate
PMMA	Poly(methyl methacrylate)
[TETAH][Lys]	Triethylenetetramine L-lysine
$[EMIM][EtSO_4]$	1-ethyl-3-methylimidazolium ethylsulfate
[EMIM][glycine (Gly)]	1-Ethyl-3-methylimidazolium amino-acetate
[EMIM][alanine (Ala)]	1-Ethyl-3-methylimidazolium (S)-2-aminopropionate
APTES	(3-Aminopropyl)triethoxysilane
BioDeg	Biodegradability
Tox	Toxicity
DOC	Dissolved organic carbon
[EHA][C5]	2-ethylhexylammonium pentanoate
[EHA][C6]	2-ethylhexylammonium hexanoate
[[BEHA][C7]	Bis-(2-ethylhexyl)ammonium heptanoate
BEHA][C5]	Bis-(2-ethylhexyl)ammonium pentanoate
[BEHA][C6]	Bis-(2-ethylhexyl)ammonium hexanoate
MAILs	Metal amino-based ionic liquids
DBU	1,8-diazabicyclo-[5,4,0]undec-7-ene
TMG	1,1,3,3-tetramethylguanidine
2D-IL	Two-dimensional ionic liquid
$[OMIM][BF_4]$	1-Methyl-3-octyl-imidazolium-tetrafluoroborate
$[BMIM][BF_6]$	1-butyl-3-methylimidazolium tetrafluoroborate
MBA	N,N'-methylene bisacrylamide
AAIL	Amino acid ionic liquid ()
[APMIM][Lys]	1-aminopropyl-3-methylimidazolium lysine
PMMA	Poly(methyl methacrylate) ()
[EMIM][TFSI]	1-Ethyl-3-methylimidazolium bis (trifluoromethylsulfonyl)imide
1B4MPTFB	1-butyl-4-methylpyridinium tetrafluoroborate ()

carbon and other pollutant reduction strategies are required. Many efforts are aimed at exploiting renewable energy sources and hydrogen for sustainable and clean power generation. In the meantime, carbon capture, utilization, sequestration, and storage (CCUS) technologies are still proposed for managing CO_2 concentrations or converting them into useful chemicals [12,13].

Although the CCUS processes look like an interesting solution [14], they are suitable only for short-term solutions. The CCUS processes have critical technical issues (regarding their energy consumption and their cost) and significant efforts are needed toward their commercialization [15]. Currently, the most acceptable technique for CAP_{CO_2} is dependent on ABTs, such as monoethanolamine (MEA) [16-18]. The CAP_{CO_2} by ABTs is governed by energy-intensive chemical reactions [17,19,20]. As such, a large quantity of heat is needed to remove CO_2 in the reproduction stage. It is anticipated that between 2.5 and 3.6 GJ of energy will be needed to release one ton of CO_2 using a 30 % MEA (aqueous) solution with an assumed 90% separation [21]. The energy demand of such a process can be reduced to 0.42 GJ/ton CO_2 if the operating pressure is increased to 150 bar. However, the CAP_{CO_2} rate under such conditions is considered very low. It was reported that approximately half of the energy used in ABTs is utilized for the regeneration of amine and the balance for pressurizing the CO_2 stream [22,23]. Other methods used for CAP_{CO_2} rely on the use of adsorbent material as a replacement for amines. However, the high energy demand and processing cost make these alternatives less feasible at large-scale [24,25].

Consequently, researchers have focused their efforts on creating innovative solvents or substances for CAP_{CO_2}. Different studies outline the use of chemical or physical adsorption or absorption, solid adsorbents, membranes, and biomimetic methods for CAP_{CO_2} [26-28]. Liu et al. [29] examined different methods for CAP_{CO_2}, with specific

attention to metal–organic frameworks (MOFs). It was determined that there isn't a single solution to the CAP_{CO_2} problem, and multiple technological solutions must be combined to overcome it. Hybrid material production also has a lot of potential. For instance, hydrophobic polymers and MOFs could be combined closely to create block co-polymers with exceptional CAP_{CO_2} capacity [30]. ILs have been investigated as emerging as materials for various energy applications and components (e.g membranes, proton conductors, and solar cells) [31,32]. They are characterized by their stability.

ILs possess high absorption capacity, they are less corrosive and biodegradable, therefore, they have been suggested as a replacement for the existing corrosive, volatile, and degraded delicate amine-solvent processes [33]. ILs are tailor-made salts comprised of ions with a low melting point of < 100 °C [34]. The usage of ILs was restricted until the late 1990 s and even then, they were only used in organic chemistry and electrochemistry. However, research by Freemantle [35] in 1998 examined the possible use of ILs as solvents for green chemistry [36,37]. The possible application of ILs has been presented in electrochemistry [38], biochemistry [39], analytical chemistry [40], catalysis [41], removal techniques [42], fluid engineering, and other applications [43-45].

The chemical and physical characteristics of ILs in addition to their low-cost synthesis and safety provided more opportunities to be used in a wide range of applications. Furthermore, their non-flammability nature and high CO_2 solubility make them an excellent choice for CAP_{CO_2} [46]. ILs are highlighted in research for their ability to substitute conventional manufacturing solvents, which are usually volatile organic compounds (VOCs) to help reduce environmental contamination. The turnability characteristics of ILs can also design solvents with specified properties [47]. Different studies introduced scientific research on CAP_{CO_2} using ILs, which resulted in an expansion of literature on this topic [48,49].

ILs could be used for CAP_{CO_2} capture under a wide variety of conditions and stream compositions. As such, the development of ILs molecular structures (protic (PILs)) or aprotic ionic liquids (AILs)) have shown outstanding efficiency of CO_2 uptake (UP_{CO_2}) using a wide variety of physical nongrafted ILs. The interactions between the anionic part of IL and CO_2 play an important role in the UP_{CO_2} and could outperform the efficiency of traditional organic solvents [50,51]. The ILs can capture CO_2 through physical absorption without chemical reaction. In this approach, the cations within the cyclic structure of ILs and the anions with long distances between O^- and N exhibited stronger electrostatic interaction and hydrogen bonding, resulting in higher UP_{CO_2}.

Therefore, the physical characteristics of ILs including solubility (S_{CO_2}), selectivity (SEL_{CO_2}) of ILs toward CO_2 as well as viscosity (VIS_{CO_2}) and volatility (VOL_{CO_2}) are important parameters in the CAP_{CO_2} process. The development of novel ILs including the synthesis of functionalized ionic liquids (FUN_{ILs}) with tuned functional groups [52] as well as supported ionic liquids membranes (SILMs) [53] have paved the way for use of such structures on a large scale for CAP_{CO_2} from industrial streams even under low CO_2 partial pressure. Cationic and anionic functionalized ILs (CAT-FUNILs) were effectively used to UP_{CO_2} from different streams with different compositions. The reversibility of ILs is another important aspect that can support their large-scale applications and recyclability [54]. Different studies have focused on developing reversible ionic liquids (RILs) that can be employed in CAP_{CO_2} processes. The developed ILs with low volatility and thermal stability showed comparable efficiency against commercial solvents for CAP_{CO_2}. The biodegradability (*BioDeg*) and toxicity (*Tox.*) of the most commonly used ILs still required further investigation to promote the green chemistry and sustainability of such technology [36,55].

As such, this work provides a thorough overview of the most recent studies and developments in the application of ILs for CAP_{CO_2} from industrial flue gases. This review also investigates a variety of viewpoints on CAP_{CO_2} using ILs [56,57], including the use of ILs in post-combustion ($Post_{com}$), precombustion (Pre_{com}) as well as oxyfuel combustion (Oxy_{com}) processes. The performance and efficiency of ILs as a CAP_{CO_2} the process was correlated to the main properties of ILs. The corresponding characteristics of ILs, selectivity (SEL_{CO_2}) and solubility (S_{CO_2}) of CO_2 as well as viscosity (V_{IL}) and cost were assessed and compared with the commercially accessible solvents (e.g., Selexol, Purisol, and Sulfinol). Moreover, the impact of specific functional groups (e.g., cations and anions) on the development and improvement of SEL_{CO_2} and S_{CO_2} in various ILs were discussed. The potential toxicity aspects as well as the biodegradability of ILs have been evaluated in this work. The reported enhancements of functionalized ILs and the corresponding developments of supported IL-membrane technology (SILM) were discussed along with the corresponding toxicity and biodegradability. The remaining challenges and future research opportunities are summarized along with a guide for producers and decision-makers to decide on the most feasible IL-based CO_2 capture method.

2. Projection of the CO_2 emissions

The energy sector contributes the most to GHG emissions among all other human activities [56]. The remaining percentages come from industrial processes, agriculture, and the burning of solid biomass to produce heat and energy. Reports showed that energy increased by 44% between 1971 and 2014 as a result of population growth and economic expansion [58]. The increase in CO_2 emissions is primarily caused by the rising global energy demand. According to a paper by Jackson et al., [59] worldwide CO_2 emissions in 2021 increased by an estimated 4.2% from 2020 to 36.2 Gt, approaching 2019 emission levels of 36.7 Gt. The energy sector accounts for 82% of those emissions, primarily from the burning of fossil fuels. Among fossil fuels burned, oil contributed up to 34% of emissions, coal was responsible for 46%, gas 19%, and the remaining 1% of emissions came from nuclear, hydro, geothermal, solar, wind, biofuels, and waste [50,56]. Together, the sectors of transportation, electricity and heat production, and fuel combustion account for about two-thirds of the world's CO_2 emissions. While road transportation accounts for the majority of CO_2 emissions in the transportation sector, coal combustion accounts for a sizeable portion of GHG emissions in the production of heat and electricity. The amount of CO_2 in the atmosphere is thus approximately 2.98×10^{15} kg, with an average CO_2 concentration of around 385 ppm [60,61]. Fig. 1 presents the industrial CO_2 emissions during the period from 1990 to 2020 [62]. The data in Fig. 1 shows that the annual CO_2 emissions increased from 3.2 ppm in 2014 to 3.6 ppm in 2016 and continue to increase through 2020. China contributes the most to global CO_2 emissions. Raising the atmospheric CO_2 concentration resulted in an increase in the CO_2 concentration at the ocean's surface, increased the dissolved inorganic carbon in water, decreased the pH of the ocean's surface, and caused ocean acidification due to gas exchange between the air and the oceans [63].

3. Conventional CAP_{CO_2} technologies

Currently, Amine-based Technologies (ABTs) are still the most common large-scale acceptable technique for CAP_{CO_2} from large-scale fossil-fired power plants [64]. The ABTs include a variety of alkanol amines chemicals (e.g., MEA, DGA, DEA, DIPA, MDEA, and TEA) that have superior reactivity with CO_2 and are considered effective for the CAP_{CO_2} [65]. The ABTs are based on reacting the flue gas in the temperature in the range of 40–60 °C with absorbent (e.g., conventional 30 wt% MEA) in the absorption tower to CAP_{CO_2} [66]. The CO_2-rich amine mixture is sent to a regeneration tower to separate CO_2 and regenerate the MEA for further use. The removed CO_2 can be either injected underground or converted to added-value products [67]. Although the ABTs are considered well-established technologies with TRL > 7, the excessive energy demand, corrosiveness, solvent degradation, and volatility are the greatest disadvantages of these methods that make them ineffective for large-scale use, including corrosiveness, which requires dilution solutions, solvent degradation in the existence of oxygen,

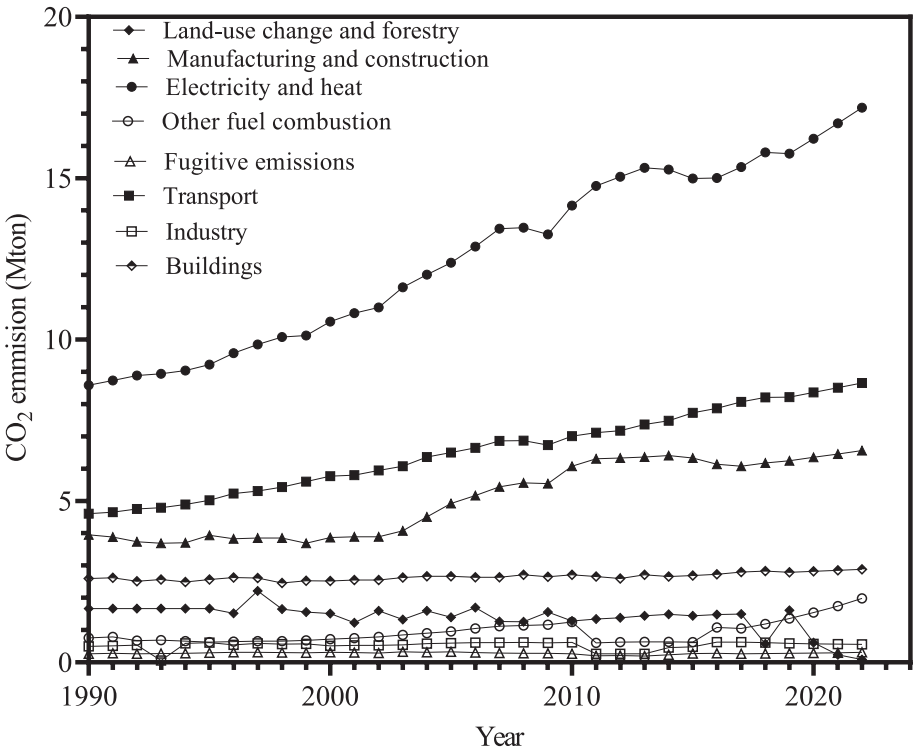

Fig. 1. Global CO_2 emissions by sector in the period 1990–2022[62].

and solvent volatility, which contaminates the environment [68]. Different studies have shown that, even though ABTs are not a particularly energy-eeffective or environmentally friendly solvent, the removal-to-uptake ratio cannot exceed 0.5 mol_{CO2}/ mol_{MEA} [69,70]. As a result, there is a big need for research work that concentrates on developing new solvents with advanced properties (low corrosivity, high CO_2 loading, less volatility, and chemical degradation) and low energy demand to be used as CAP_{CO_2} processes [71].

The $Post_{com}$, Pre_{com} and Oxy_{com} are considered the most common processes used for CAP_{CO_2} are [72]. The properties of $Post_{com}$, Pre_{com} and Oxy_{com} are separate and have specific CAP_{CO_2} requirements. The $Post_{com}$ is considered the cheapest technology for CAP_{CO_2} that could be used in old and new systems. On the other hand, the Pre_{com} and Oxy_{com} techniques could be implemented only in new power plants [73]. Investing in the Pre_{com} technique remains significant in comparison to Pre_{com} and Oxy_{com}.

The $Post_{com}$ process is the first choice for CAP_{CO_2} [74]. It is commonly applied as CAP_{CO_2} in conventional fossil fuel-fired power stations. In the $Post_{com}$ process, fuel is completely burned in a single stage and the free heat is utilized to create high-pressure steam, which is then used to produce electrical energy. As such, the removal method is capable of managing a wide variety of conditions. The flue gas from the boiler is comprised of large quantities of material that is sorted in the coal elimination stage. If the flue gas contains sulfur it passes through limestone slurry to remove it and generate gypsum. The $Post_{com}$ is characterized by a clean flue gas with a CO_2 mass fraction in the range of 10 to 16%, high selectivity to CO_2, and low-pressure CO_2, which adds substantial costs for pressurization [75].

In the Pre_{com} technique, fuel is vaporized, mixed with oxygen, and stripped with steam to generate syngas (CO and H_2). The mixture is fed to a water–gas-shift (WGS) reactor to produce H_2 and CO_2. The CO_2-rich gas mixture is separated, transported, and ultimately sequestered. While the H_2-rich stream is used as fuel to generate electricity. The high CO_2 partial pressure (P_{CO_2}) produced from Pre_{com} technique enhances CO_2 removal while reducing the costs of gas pressurizing. However, additional costs are required to maintain high pressure in the WGS reactor [76].

The Oxy_{com} the technique has shown potential as CAP_{CO_2}, however, with slow progress. In this process, concentrated pure oxygen is mixed with fuel and burned to generate the necessary heat and produce high-pressure steam (HPS) and electricity. The flue gas (H_2O and CO_2) is stripped and partially reused to manage the temperature in the boiler. The outlet concentrated CO_2 stream can be later injected underground or converted into other products. The use of pure oxygen eliminates the need for the N_2 separation stage. The Oxy_{com} technique can effectively capture CO_2 from flue gases at a low cost. However special types of boilers are required to tolerate the high temperatures resulting from using pure oxygen [77].

4. CO_2 capture (CAP_{CO_2}) using ionic liquids

Many ILs have great potential for CAP_{CO_2}. The ILs can have two different molecular structures (1) protic ionic liquids (PILs)) that can donate a proton and (2) aprotic ionic liquids (AILs)) that cannot donate a proton. Fig. 2 illustrates some examples of PILs and AILs used for CAP_{CO_2}, where the R groups are common alkyl groups. The primary focus of the early research on CAP_{CO_2} using ILs is the efficiency of CO_2 uptake (UP_{CO_2}) using a wide variety of physical nongrafted ILs. It was reported that the interactions between the anionic part of IL and CO_2 play an important role in the UP_{CO_2} [50,51] in comparison to traditional solvents such as toluene and n-hexane. Standard IL, such as [emim][Tf_2N] showed a high UP_{CO_2} under different operational conditions, while traditional molecular solvents demonstrated significant UP_{CO_2} only at high to medium pressures [78]. As the bubble-point pressure increase by increasing the operating pressure and the CO_2 mole fraction, this can significantly affect the UP_{CO_2}. This special performance is communal for CO_2-IL schemes and is categorized as type III fluid-phase performance [79]. A more reasonable evaluation of $CO_2 - IL$ schemes is liquid polymers with high molecular weight (HMW). Different anion-based PILs (e.g., [DBUH][2-OP], [DBUH][3-OP], [DBUH][4-OP], [TMGH][2-OP], [TMGH][3-OP], and [TMGH][4-OP]) containing different functional groups were tested for UP_{CO_2} at 313.2 K and 101.3

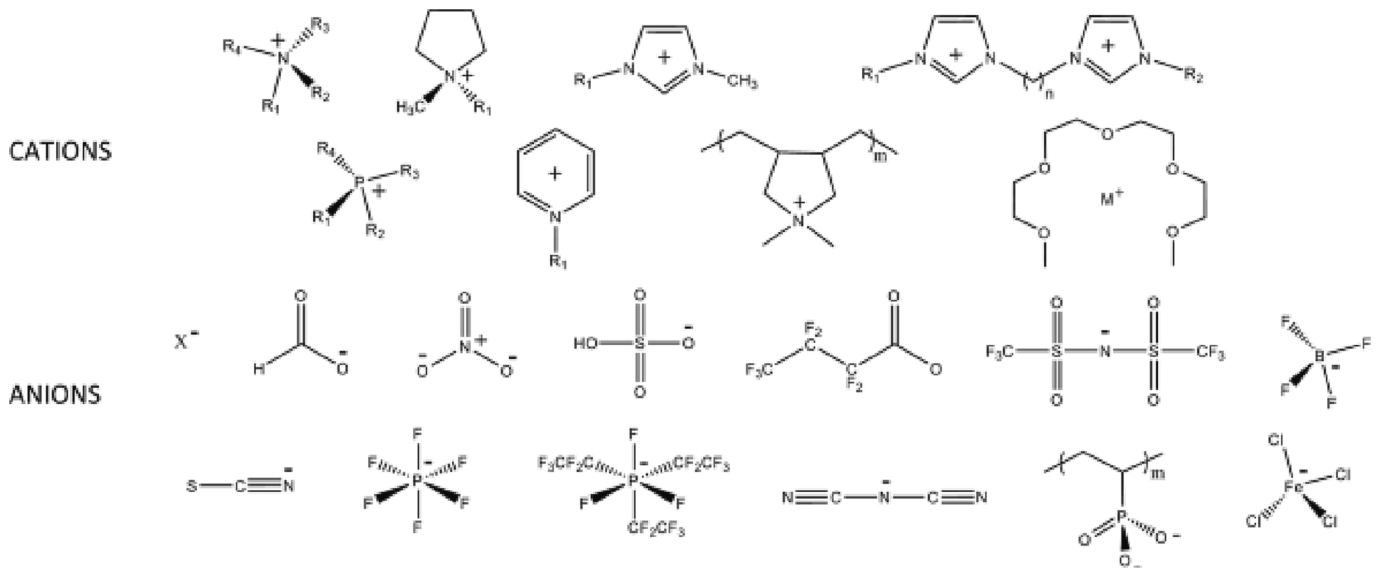

Fig. 2. Samples of protic (PILs)) and aprotic(AILs) ionic liquids used for CAP_{CO_2}. Print with permission from [81].

kPa. It was reported that these ILS exhibited higher UP_{CO_2} due to the presence of strong electrostatic interaction and hydrogen bond as explained before. The UP_{CO_2} follows the order [4-OP]$^-$> [3-OP]$^-$> [2-OP]$^-$ and [DBUH]$^+$> [TMGH]$^+$ [80].

CAP_{CO_2} by Ionic Liquids.

The most common approach for the CAP_{CO_2} by ILs is through physical absorption without chemical reaction. In such an approach, the physical characteristics of ILs including solubility (S_{CO_2}), selectivity (SEL_{CO_2}) of ILs toward CO_2 as well as viscosity (VIS_{CO_2}) and volatility (VOL_{CO_2}) play an important role. Table 1 illustrates the common characteristics of ILs used in CAP_{CO_2} [81].

5. Characteristics of ILs

5.1. Solubility of CO_2 in ILs (S_{CO_2})

Anionic ionic liquids (AILs) have higher UP_{CO_2} compared with PILs. Aki et al. [82] confirmed that AILs play a primary role in CAP_{CO_2}, while PILs play a secondary role. This was related to the ability of AILs to form strong Coulombic interactions that help form a network to increase the dissolution of CO_2 and enhance the UP_{CO_2} [83]. The formation of such force helps the CO_2 to locate within the ILs interstices, increases the S_{CO_2} and the observed UP_{CO_2} [84]. Kazarian et al. [85] showed through in-situ ATR-IR spectroscopy testing that the anionic properties of [BF_4] and [PF_6] S_{CO_2} enhanced the S_{CO_2} and therefore the UP_{CO_2} efficiency. It was highlighted that the CO_2-IL interaction follows Lewis acid (AIL)-base (CO_2) interactions. Therefore, the stronger the basic properties of [BF_4] helped in identifying why the S_{CO_2} in [BF_4] is higher than in [PF_6]. Similarly, stronger basic properties explained the high S_{CO_2} in [bmim][PF_6] compared to [bmim][BF_4]. Other studies suggested that the Lewis acid-base (CO_2) interactions alone could not describe the S_{CO_2} and the capability of AILs for UP_{CO_2}. Therefore, free volume of ILs (IL_{FV}) mechanism, which can explain the variation in the dispersing of CO_2 within the ILs was connected with the S_{CO_2} [86,87]. The IL_{FV} mechanism is based on the fact that when CO_2 is introduced to the ILs the volume of free cavities does not considerably change until the saturation limit of CO_2 is reached. Researchers showed that CO_2 occupies the vacant site within [bmim][PF_6] and arranges over the anion part of [PF_6] [88,89]. The addition of different anions to the PIL increased the S_{CO_2} [90,91]. The tests which were carried out at 30 °C showed that the selectivities of gases in ILs are ranged as $S_{NO_3} < S_{SCN} < S_{MeSO_4} < S_{BF_4} < S_{DCA} < S_{PF_6} < S_{TF_2N} < S_{\text{Methide}} < S_{T7F_{15}CO2}$ [92]. Similar trends were reported before by Maiti [93] and Sistla [94] during the screening of the S_{CO_2} of different ILs using COSMO-RS model. It was highlighted that the ILs that contain fluoride have higher ionic properties and exhibited higher S_{CO_2} compared with ILs without a fluoride group. The anion-fluorination trend was also examined with the most common cationic IL ([bmim]). The reported trend showed that the S_{CO_2} improves by increasing the number of fluoride groups within the structure. The S_{CO_2} was arranged as follows: $S_{BF_4} < S_{TfO} < S_{TfA} < S_{PF_6} < S_{TF_2N} < S_{\text{Methide}} < S_{T7F_{15}CO2} < S_{eFAP} < S_{bFAP}$. In similar manner, it was observed that the addition of an extended fluoroalkyl chain to AILs, such as [FAP] enhance the S_{CO_2} [91,95]. The COSMO-RS tests helped in the understanding CO_2 dissolution in ILs [96]. To achieve this, a large number of ILs were tested and Henry's law was effectively linked to the S_{CO_2} and the corresponding enthalpy of dissolution in ILs. It was confirmed that the S_{CO_2} is linearly proportional to the mixture exothermicity. Furthermore, the intermolecular interactions between fluid phases, including hydrogen bonds, electrostatic forces, and van der Waals forces were calculated and correlated to the S_{CO_2} in ILs [97]. It was discovered that van der Waals forces debate and control the UP_{CO_2} by increasing CO_2 dissolution in ILs. Because the hydrogen bond contribution was insignificant, electrostatic interactions played a minor role in the enthalpy of dissolution [97]. According to these results, Palomar et al. [97] conducted a COSMO-RS to identify new ILs with an improved van der Waals forces and thus achieve high UP_{CO_2}. Tests howed that adding bromine to ILs (e.g [emim][PBr_6]) improved the S_{CO_2} and UP_{CO_2}. Hospital-Benito et al. [98] used DFT/COSMO-RS quantum chemical calculations to developed different N–Heterocyclic Anion-based Ionic Liquids (AHA-ILs) that achieved UP_{CO_2} Cyclic capacity in the range 0.39 to 1.73 mol/kg under reasonable enthalpy in the range − 43 and − 54 kJ/mol.

Table 1
Common properties and characteristics of ILs [81].

Property	Common Characters
Vapor Pressure	Negligible
Conductivity	Good (<10 μs/cm)
Viscosity	Workable (<100 cp)
Thermal stability	Very stable
Freezing temperature	<100℃
Liquidous temperature	>200℃
Polarity	Average
Solvency	Strong
Characteristics as Catalysis	High especially with organic compounds
Salt ions	Large-size anions and cations

The S_{CO_2} in ILs was also tested by adding ammonium, cholinium, pyridinium, pyrrolidinium and phosphonium, and imidazolium cations with anionic [Tf_2N] [99]. Cation fluorination, such as [$C_6H_4F_9$mim] can substantially enhance the S_{CO_2} in comparison to anion fluorination [100]. It was also observed that the presence of long alkyl chains (LAC) in the phosphonium cation [$P_{666,14}$] enhances the S_{CO_2} [101]. Combining ILs with conventional bis(trifluoromethyl sulfonyl)amide [Tf_2N] anions also enhance the S_{CO_2}. Different studies showed that the S_{CO_2} enhance by increasing the length of LAC. The COSMO method explained the acidity of ILs by their structure. ILs can form a hydrogen bond in the C_2 position of the imidazolium ring, which has a comparatively high positive charge. Therefore, more UP_{CO_2} can occur on this site by exchanging with hydrogen [94,102,103]. Both experimental and molecular simulations confirmed that when a methyl group took the place of the H proton in the C_2 site, the S_{CO_2} slightly decreased [82,104,105]. Henry's constant of S_{CO_2} in [bmim][PF_6] at 25 °C was found to be 53.4 bar, while it is 61.8 bar in [bmmim][PF_6] with methyl grouped substituted [104]. The impact of hydrogen bond donors on the CO_2-epoxide cycloaddition reaction was discussed by Jiang et al. [106]. It was proposed that ILs, such as PIL-COOH@MIL-101 have an efficient catalytic performance during the CO_2 cycloaddition reaction, achieving conversion of 92.7% at 70 °C and 1.0 MPa in 2.5 h. The enhanced activity was attributed to the synergistic effects of Lewis acidic on the IL centers, carboxyl group, and the presence of nucleophilic halogen ion, such as Br-, in addition to the high surface area (1178 m^2/g) and good CO_2 affinity.

Although many molecular simulations have been used to examine the S_{CO_2} in Ils, very little research has been done on developing the S_{CO_2} isotherms. Rapid testing approaches, such as COSMO help select an ideal IL for CAP_{CO_2} from flue gases. Numerous additional approaches that use viscosity or surface tension properties have also been used to determine the solubility of gases in Ils [107-109]. The regular solution theory (RST) can be used to determine the solubility of gases in ILs at low pressures [110]. The RST correlated the solute activity coefficient (γ_1) with the liquid molar volume ($\widetilde{V_1}$) and the variation in the parameters of solubility of solute and solvent (δ_1 and δ_2), respectively, as shown in Eq. (1).

$$RT\ln\gamma_1 = \widetilde{V_1}\Phi_2{}^2[\delta_1 - \delta_2]^2 \quad (1)$$

Once the RST factors are identified the total solubility isotherm can be determined[111]. The δ_2 can be undetermined and/or altered to fit experimental isotherms. Recently, an exact value of δ_2 was determined using the vaporization enthalpies as per the correlation $\delta_2 = (\Delta H_{vap}U_2/V_2)$. However, it was observed that the experimental values of δ_2 resulted in a bad prediction of the S_{CO_2} in [hmim]-[Tf_2N] when using RST. The weak behavior of the RST when using real solubility rather than related solubility factors to define the S_{CO_2} is unremarkable. Typically, adding CO_2 to Ils at a low pressure displayed negative deviation from ideality as outlined by Raoul's law. As a result, the γ_{CO_2} for the Ils is<1. However, the RST can define mixtures with positive changes from ideality.

The S_{CO_2} based on mole fraction was also used in experimental and simulation to determine UP_{CO_2}. Different studies suggested that entropy impacts and controls the physical UP_{CO_2} by ILs [112] As such, plotting the S_{CO_2} as a function of molality (m) under specific pressure exhibit widespread curve. This allow for establishimg a correlation (see Eq. (2) for S_{CO_2} in Ils as a function of pressure in the temperature range 25–93 °C.

Different studies used the model in Eq. (2) to identify the S_{CO_2} in Ils [82,113,114]. However, many Ils showed a significant deviation from Eq. (2) [115,116]. For instance, formats (m-2HEAF) and acetates (m-2-HEAA) prompted the S_{CO_2} via the development of electron donor–acceptor (EDA) compounds and do not follow Eq. (2). Other Ils with subsequent anions (e.g., [SCN], [xSO_4], [NO_3], [doc], and [mp]) as well as [bmim][BF_4]. Several [PF_6], [TfO], and [DCA] do not follow such standard correlation, suggesting that the proposed model needs further enhancement.

$$P = m_i{}^0 e^{6.8591-2004.3/T} \quad (2)$$

Several researchers noted that the molecular weight of IL (MW_{Ils}) has a major contribution to the S_{CO_2} [114,117,118]. Subsequent studies highlighted how the S_{CO_2} improves by increasing the MW_{Ils}, though initially the solubility was thought to be part of the molarity (mol/m^3). The S_{CO_2} data is in agreement with the data reported in the literature [114,117,118]. In generally the S_{CO_2} data was conveyed in molarity [99,119,120]. The plot of pressure vs. molarity for several Ils produces nearly straight lines. The slops these lines can be used to calculate the molarity-based Henry's constants. Henry's coefficients (H_c) are then plotted against the MW_{IL}. The observed trends show that the H_c of S_{CO_2} decrease by increasing the MW_{Ils}.

The free-space method is another method used to evaluate the S_{CO_2} in ILs. This method is based on the molar-free volume of ILs (IL_{MFV}). It was observed a strong correlation between H_c and the IL_{MFV}, where the H_c decreased by increasing the IL_{MFV}. Thus, the free-space method has been used to determine the S_{CO_2} of different Ils [110,119-121]. Zhao et al. [122] developed a correlation based on Bondi rules [123] that can help todetermine the Van der Waals molar volume (IL_{VDMV}) and consequently approximate the IL_{MFV}. The free-space method was used to accurately evaluate the IL_{VDMV} of 677 organic complexes [122]. Moreover, the IL_{MFV} was used by many researchers to calculate H_c of different Ils [99,119,120] and link them with the S_{CO_2}. It was noticed that the IL_{MFV} relied on the aromatic imidazolium and the pyridine rings as well as the nonaromatic pyrrolidine ring. Moreover, it was confirmed that the IL_{MFV} seems to increase with the increase of MW_{Ils}.

Shannon et al. [124] noted that the IL_{MFV} controls the S_{CO_2} and SEL_{CO_2} in Ils. It was observed that the normalized S_{CO_2} is correlated with $(IL_{MFV})^{-0.5}$. Conversely, the CH_4 and N_2 solubility demonstrated a linear reliance on the IL_{MFV}. As such, the S_{CO_2} improves with an increased IL_{MFV} and MW_{IL}. These outcomes support the findings reported by Carvalho and Coutinho [115] who demonstrated that entropic impacts control the S_{CO_2} in Ils instead of solute/solvent interactions. The solubility trends as a unctionn of molarity or molality alter when the trends are formed on a mole fraction basis. The single enduring trend is the S_{CO_2} in fluorinated ILs is greater than in nonfluorinated Ils. Besides controlling the free-space method, the aforementioned trend indicates that interactions between solute and solvent are crucial. It is important to highlight that the S_{CO_2} is not assessed on the mole fraction basis because of the powerful impact of molar volume. From a usage perspective, it is further attractive to evaluate the solubility on a molality basis or per volume solvent (molarity) [125]. Experimental data on the S_{CO_2} for imidazolium-based ILs, phosphonium, pyridinium, and pyrrolidinium ILs are illustrated in Table 2 and 3, respectively.

5.2. Density of ILs

ILs are denser than water except for pyrrolidinium dicyano-diamide and guanidinium, which have densities ranging from 0.90 to 0.97 g/cm^3. It was reported that the density of ILs is correlated to its structure and decreases by increasing the length of the alkyl chain and the number of carbon in that chain. Increasing the temperature can decrease the density of IL. Fig. 3 shows that as the temperature rises, the density of three commonly used Ils decrease. Unlike traditional organic solvents, an increase in the number of carbons in the alkyl group increases the viscosity of ILs due to the presence of hydrogen bonding and van der Waals interactions, as will be explained later. Experimental results showed that the best model to predict the density of Ils is the Tait equation [132].

5.3. Selectivity of ILs toward CO_2 (SEL_{CO_2})

The S_{CO_2} data is not sufficient to assess the removal efficiency of CO_2

Table 2
The S_{CO_2} in different imidazolium-based ILs [56].

Ionic Liquid	Temp. (K)	Pressure (bar)	$S_{CO_{2,max}}$ (CO_2/mol_{IL})	Ref.
[bmim][NO_3]	–	–	0.442	[82]
[bmim methide]	–	–	0.761	[82]
[bmim] [Tf_2N]	–	–	0.681	[82]
[bmim] [TFO]	–	–	0.641	[82]
[bmim] [bF_6]	–	–	0.640	[82]
[bmim] [BF_4]	–	–	0.520	[82]
[bmim] [NO_3]	–	–	0.475	[82]
[bmim] [BF_6]	283–348	0.096–19.99	0.379	[126]
[bmim] [DCA]	298.15, 333.15	1–120	0.550	[82]
[C_8mim] [PF_6]	–	–	0.755	[113]
[C_8mim] [PF_4]	–	–	0.513	[113]
[bmim] [PF_6]	313.15, 333.15	0.97–92	0.729	[113]
[bmim] [PF_4]	–	–	0.364	[113,126]
[bmim] [PF_6]	293–393	1–97	0.555	[127]
[hmim] [FEP]	283.15, 298.6	0.297–18.1	0.517	[95]

Table 3
The experimental data for S_{CO_2} in different ILs.

Ionic Liquid	Temp. (K)	Pressure (bar)	$S_{CO_{2,max}}$ (CO_2/mol_{IL})	Ref.
[$N_{(1)888}$] [Tf_2N]	–	–	0.364	[128]
[$N_{(6)222}$] [Tf_2N]	–	29	0.034	[128]
[hmpy] [Tf_2N]	283	1–10	0.200	[128]
[$P_{(4)113}$] [Tf_2N]	–	–	–	[129]
[$P_{(6)113}$] [Tf_2N]	–	–	–	[129]
[$P_{(10)113}$] [Tf_2N]	–	–	–	[129]
[$P_{(4)111}$] [Tf_2N]	–	–	–	[129]
[$P_{(6)111}$] [Tf_2N]	–	–	–	[126]
[$P_{(10)111}$] [Tf_2N]	–	–	–	[129]
[$P_{(4)111}$] [Tf_2N]	293.2–363.2	1.06–375	0.879	[130]
[N-buby] [BF_4]	313.15, 333.15	0.97–91.9	0.518	[82]
[$P_{(2)444}$] [DEP]	–	–	0.001	[129]
[$P_{(14)666}$] [Cl]	303.15	1	0.033	[129]
[$P_{(14)666}$] [DCA]	–	–	0.034	[129]
[$P_{(14)666}$] [Tf_2N]	283	1–10	0.033	[129]
[hmim][FEP]	283.15–323.2	0.3–18.1	0.517	[131]
[bmpyrr][FEP]			0.498	[131]
[ETT][FEP]			0.497	[131]
[bmim][PF_6]	293–393	1–97	0.379–0.729	[127]
[bmim][BF_4]			0.364	[56]
[C8mim][PF_6]			0.755	[56]
[C8mim][BF_4]			0.513	[56]
[bmim][NO_3]			0.708	[56]
[emim] [$EtSO_4$]			0.579	[56]
[N-bupy][BF_4]			0.423	[56]
[C2-mim] [Tf_2N]	301–344.4	10–43	0.761	[56]
[C6-mim] [Tf_2N]			0.833	[56]
[C8-mim] [Tf_2N]			0.845	[56]

by IL, instead, the selectivity of IL to CO_2 (SEL_{CO_2}) provides the additional necessary information. While data on S_{CO_2} is accessible in the literature, information on SEL_{CO_2} is minimal. When discussing the CAP_{CO_2} from flue gases, the selectivities, in general, are mostly related to the composition of flue gas as well as the ratio of different components (i.e., CO_2/H_2, CO_2/CH_4, and CO_2/N_2). Sometimes flue gases can include other impurities, such as SO_x, H_2S, and even CO. Therefore, the SEL_{CO_2} is more important than the S_{CO_2}. Different studies have compared the S_{CO_2} of ILs with other flue gas constituents. It was observed that the S_{CO_2} in IL [hmpy][Tf_2N] at 298°K is comparable withand the S_{SO_2} followed by $S_{C_2H_4}$, $S_{C_2H_6}$, S_{CH_4}, S_{O_2}, and S_{N_2}, respectively [128,134,135].

In general, the fuel gas from fossil fuel-fired power plants contains 8–10% CO_2, 18–20% H_2O, 2–3% O_2, and 67–72 % N_2. The high SEL_{CO_2} sugest that [hmpy][Tf_2N] could be used as an efficient CAP_{CO_2} of these flue gases. The observed high solubility of hydrocarbons (e.g., $S_{C_2H_4}$, $S_{C_2H_6}$, and S_{CH_4}) in IL, such as [hmpy][Tf_2N] could slightly lower the SEL_{CO_2} and therefore the UP_{CO_2}. SO_2 might also compete with CO_2 during the CAP_{CO_2} using [hmpy][Tf_2N]. Kumełan et al. [136] showed that the S_{CO_2}, $S_{C_2H_4}$, and $S_{C_2H_6}$ in ILs increase by decreasing the operating temperature. Nevertheless, the S_{CH_4} and S_{O_2} in [bmim][PF_6] do not dependent on the temperature change. Cooling of the flue during the CAP_{CO_2} is unlikely. Therefore, ILs with high S_{CO_2} under high temperature is highly required. Carvalho and Coutinho [137] on the other hand, showed that the S_{CH_4} in phosphonium, ammonium, and imidazolium ILs slightly change with temperature. The particularities of the S_{CH_4} in ILs was found to vary beyond the temperature dependence [115]. The S_{CH_4} slightly increase by increasing the temperature, however, it shifted or affected by the IL polarity. The selectivities of different ILs toward H_2S/CH_4 or CO_2/CH_4 could be correlated using the Kamlet-Taft β factor that is based on hydrogen bond donating/ accepting as well as the polarization characteristics of the solvent. Kumelan et al. [136,138] disclosed that the S_{CO} and S_{H_2} in [bmim][PF_6] and [hmim][Tf_2N] are notably lower than S_{CO_2} suggesting that this IL has high SEL_{CO_2} and promising UP_{CO_2}. In addition, the S_{H_2} in [bmpy][Tf_2N] and [hmim][Tf_2N] was found to increase by increasing the temperature [114,139]. Although the S_{CO_2} in [bmim][PF_6] declines by increasing the temperature, the S_{CO} was not affected by the temperature increase. Similarly, the S_{CO} in [bmim][CH_3SO_4] increased by increasing the temperature [140]. The solubility of numerous gases in [bmim][PF_6] and [bmim][BF_4] under low pressure was reported by Jacquemin et al. [141,142]. It was

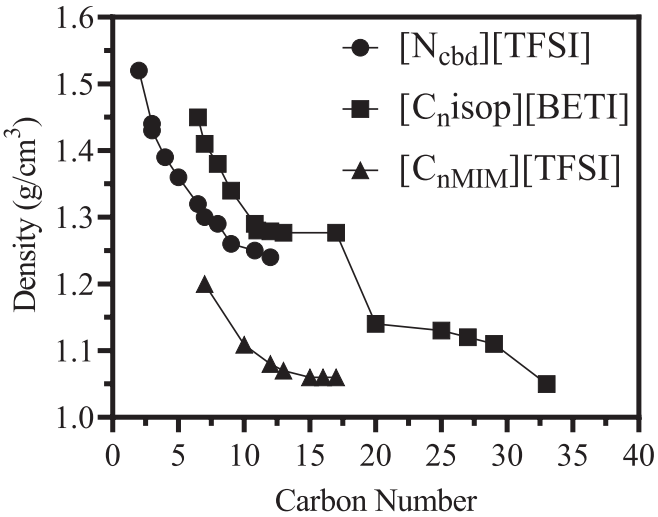

Fig. 3. Change of ils density as a function of carbon number. adapted with permission from reference [133].

observed that the S_{H_2} was lowest in both ILs, while the S_{CO_2} was the highest. This confirmed the previous trend related to UP_{CO_2} and the increase in S_{H_2} by decreasing temperatures. Therefore, the [bmim][PF_6] and [bmim][BF_4] were highly recommended as CAP_{CO_2} since the solubilities of flue gases are arranged as $S_{H_2} < S_{CO} < S_{N_2} < S_{O_2} < S_{AR} < S_{CH_4} < S_{C2H_6} < S_{CO_2}$. Jacquemin et al. [143] tested the impact of adding cations part too the IL on the S_{H_2}. When cations, such as [N_{4111}], [bmim], and [emim] were added to the anion [Tf_2N], the S_{H_2} slightly increased. The high S_{H_2} was achieved by [N_{4111}]- [Tf_2N] combination. Additionally, in such combination it was observed that the S_{H_2} decreased with temperature, which is different from [hmim]-[Tf_2N], [bmpy]-[Tf_2N], and [bmim]-[PF_6] combinations.

Shiflett and Yokozeki [144] estimated that the SEL_{CO_2} in [bmim][PF_6] under normal operating conditions can be as high as 30–300, which is higher than new polymeric membranes (10–30) [145]. The calculated SEL_{CO_2} in [bmim][$MeSO_4$] and [bmim][PF_6] using the EOSs for gas mixture that contains CO_2/H_2S gas was in the range 3.2 to 4. [146]. The results demonstrated a high competition between the two gases causing a low SEL_{CO_2} in the [bmim][PF_6]. It was also observed that the SEL_{CO_2} in the [bmim][$MeSO_4$] system depends on the CO_2/H_2S molar ratio [146,147]. High to medium mol ratio reported SEL_{CO_2} in the range 10 to 13 [146,147]. The solubility of H_2, O_2, CO, N_2 were also estimated in similar ILs and the results showed wide variations in the reported values [141,148,149]. For instance, the H_C of oxygen in [bmim][PF_6] was found to be 650 ± 425 MPa at 283 K, whereas the value decreased to 51.5 ± 0.6 MPa at 283 K [150 136,138].

The gases' polarity was correlated to their solubilities in IL. Simple gases often interact unconvincingly with ILs, whereas gases with electric quadrupole moment, such as S_{CO_2} and S_{C2H_4} exhibited higher solubilities [151,152]. The general solubility sequence was reported as before. Camper et al. [153,154] demonstrated how the real solubility of gases in ILs was associated with the IL_{MFV} and how standard selectivities for CO_2/CH_4 and CO_2/N_2 improved by decreasing the IL_{MFV}. Finotello et al. [154] assessed the SEL_{CO_2}, SEL_{N_2}, and SEL_{CH_3} in pure [bmim][Tf_2N] and [bmim][BF_4] as well as in mixtures of these ILs. It was highlighted that the maximum *SEL* of these gases was achieved by mixing 5 mol % [bmim][Tf_2N] with balanced [bmim][BF_4]. The SEL_{CO_2} by imidazolium-based ILs grafted with oligo(ethylene glycol) from gas mixtures of CO_2, CH_4 and N_2 was higher than the SEL_{CH_4} and SEL_{N_2} [155]. Carlisle et al. [156] found comparable outcomes in the system that used nitrile-grafted ILs.

Mahurin et al. [157] assessed the SEL_{CO_2} of a mixture of CO_2/N_2 in pyrrolidinium, imidazolium, and pyridinium ILs grafted with a benzyl group. The reported SEL_{CO_2} was in the range 22 to 33, suggesting higher UP_{CO_2}. Typically, determining the solubilities of the mixed gas is more complicated, thus there is limited mixture solubility data outlined in the literature. Hert et al. [158] examined some of the initial solubilities of mixed gas, particularly (O_2 CO_2 and CH_4) in the [hmim][Tf_2N] IL. Moreover, Shi and Maginn et al. [159] reported minimal to no development of S_{O_2} in the existence of CO_2. Modified experiments on CO_2/O_2 confirmed the results, meaning that the estimated SEL_{CO_2} of CO_2/O_2 mixture have values close to ideal [160].

The S_{CO_2} and S_{H_2S} in ILs [bmim][$MeSO_4$], [bmim][PF_6], and [omim][Tf_2N] were examined by Shiflett et al. [146,161] and Jalili et al. [162]. It was concluded that the S_{CO_2} and S_{H_2S} in [bmim][PF_6] and [bmim][$MeSO_4$] rely on the feed composition and temperature. Reported solubility values at 298.15 K were in the ranges of 1 to 10 and 1 to 4, respectively. The same study determined the SEL_{CO_2} in [omim][Tf_2N] at 303.15 K IL to be ~3.

In the case of removing CO_2 from natural gas, which operates at high pressure, the SEL_{CO_2} would not be collocated with the performance of the CAP_{CO_2} process. As previously noted, in the Pre_{com} method, the SEL_{CO_2} and SEL_{H_2} are both high. Therefore, the UP_{CO_2} from natural gas should be correlated under real operating conditions. The SEL_{CO_2} and SEL_{H_2} have been mostly studied [144,159,163]. For instance, Yokozeki and Shiflett [144] compared the SEL_{CO_2} with the SEL_{H_2} in [bmim][PF_6] and demonstrated that both values decline by increasing the temperature and pressure. Additionally, Kim et al. [164] demonstrated high SEL_{CO_2} in the CO_2/N_2 mixture treated by [hmim][Tf_2N]. Small amounts of N_2 were absorbed on the IL, which indicates an excellent UP_{CO_2} and high performance.

In summary, the critical factor in removing CO_2 by IL is highly dependent on the composition of gas and mainly the CO_2/N_2 ratio. The SEL_{CO_2} in different ILs is higher than the SEL_{N_2} suggesting excellent CAP_{CO_2} efficiency. In the Pre_{com} method, presuming the separation of CO_2 after the WGS reaction, the important removal is CO_2/H_2 ratio. While standard SEL_{CO_2} in a mixture of CO_2/H_2 in ILs is comparatively high, the actual *SEL* is expected to be smaller than standard *SEL* at greater temperatures. This is because the S_{H_2} in ILs improves by increasing the temperature, though the reverse is true for CO_2. Many pollutants should be removed during natural gas sweetening, but the most frequent removals are CO_2/H_2S and CO_2/CH_4. The standard *SEL* for CO_2/CH_4 in ILs is similar to the standard natural solvents, however, the real *SEL* for CO_2/CH_4 in ILs is estimated to be less than the standard *SEL*. Moreover, the standard *SEL* cannot be anticipated for the mixture of CO_2 and H_2S because the S_{CO_2} is substantially reduced due to H_2S, which is considerably more solvable in ILs. Thus, both gases can be eliminated instantaneously, however, this is not beneficial because an extra stage may be needed for removing CO_2 from H_2S.

5.4. Viscosity of ionic liquids (Vis_{IL})

The viscosity of ILs (Vis_{ILs}) is a crucial factor during the CAP_{CO_2} because high Vis_{IL} can cause a decrease the mass transfer and might restrict any possible UP_{CO_2} [165]. ILs viscosity and density are affected by the quantity of water and other pollutants in the ILs [99]. Several ILs produce extremely viscous gel-like materials and thus exhibit low UP_{CO_2} efficiency. With fortune, ILs properties can be tuned to create a wide Vis_{IL} range. Different studies elaborated on the relationship between Vis_{IL} and temperature of commonly used ILs [166-168]. It was reported that most ILs follow Arrhenius law that linearly correlates the Vis_{IL} with 1/T. Deviation from Arrhenius law was generally explained by the Vogel-Fulcher-Tammann (VFT) equation [169]. Zhao et al., [170] developed three novel functionalized ILs [N8881][NIA], [N8881][For] that exhibit low viscosity, high UP_{CO_2} capacity and excellent recyclability. The capacity was ordered as [N8881][NIA] > [N8881][For] > [N8881][Ac].

The pressure reliance of the Vis_{IL} exhibits significant variations from the normal performance of molecular solvents [171,172]. It is clear that the Vis_{IL} is greater than traditional solvents, such as alcohols, water, or acetonitrile. Several studies have attempted to create ILs with low viscosities by controlling the cations and anions [166-168]. The viscosity of ammonium, pyridinium, imidazolium, phosphonium, and pyrrolidinium ILs with a familiar [Tf_2N] anion was also investigated at 298 K. The Vis_{IL} improvement for the aforementioned action is as follows: imidazolium [hmim] < pyridinium [hmpy] < pyrrolidinium [hmpyrr] < phosphonium [P_{2228}] < ammonium [N_{2228}] [166-168].

Gardas and Coutinho [173,174] assessed the transport and thermophysical properties of ILs, including isothermal compressibility, viscosity, isobaric electrical expansivity, conductivity, thermal conductivity, and refractive index. This group examined the viscosities of 29 ILs with an average percentage difference of 7.7% and the highest difference of 28%. Recently, Zailani et al., [175] prepared ammonium-based—PILs ([EHA][C5]), [EHA][C6], [EHA][C7], [BEHA][C5],[BEHA][C6]) and [BEHA][C7] with an excellent UP_{CO_2} even at high pressure of 29 bar. results showed that [BEHA][C7] had the highest UP_{CO_2} capacity of 0.78 mol at 29 bar. The UP_{CO_2} capacity can be ordered as [C5] < [C6] < [C7]. Maginn [160] provided a comprehensive review of IL dynamics and molecular simulations of ILs. While simulations primarily separate the slow dynamics of IL systems, they can also achieve very short period scales to measure credible viscosities [160]. During chemical reactions,

viscosity is significant because, in dispersion-controlled reactions, the constant rate would reverse compared to the solvent viscosity [165]. Thus, several reactions are sluggish in ILs in comparison to traditional solvents owing to high IL viscosity. The cation and anion self-diffusion coefficients (D) at 298 K are in the order of 10–11 m^2/s, in comparison to 10–10–10–9 m^2/s for simple molecular liquids [160,165].

Hou and Baltus [176] used a separate correlation for CO_2 diffusivity in imidazolium ILs and took into consideration the IL molar mass, viscosity, density, and temperature. Similarly, Ferguson and Scovazzo examined gas diffusion in phosphonium ILs [177]. Studies discovered that the viscosity of the phosphonium ILs was inversely related to the diffusivity. Moreover, the gas diffusivity in phosphonium ILs is connected to the solvent viscosity, the molar volume of the solvent, and the solute. In contrast, Condemarin and Scovazzo [128] assessed gas diffusivities in ammonium ILs. The authors found that the gases' diffusivity was dependent upon the solvent viscosity. These studies demonstrate how the diffusivity varies according to the type of ILs. Additionally, the Stokes-Einstein equation exhibited how the diffusivity of gases in ILs is less reliant on the viscosity than expected. Though, this is questionable because the Stokes-Einstein equation usually indicates where a great solute particle disperses in a solvent for relatively small molecules [178].

5.5. Volatility of ionic liquids (VOL_{IL})

Typically, ILs are regarded as materials with low vapor pressure (Pv), however, this idea was changed by Earle et al. [179] who showed that various commonly used AILs could be distilled at 300 °C under vacuum pressure without any sign of noteworthy decomposition. The [hmim][Tf_2N] ILs can be distilled at 169 °C and 0.08 bar without significant decomposition. Different authors were challenged to find an empirical correlation between the ILs' boiling point (Pb), Pv, vapor phase, enthalpy of vaporization (ΔH_{vap}), and boiling temperature (Tb) [137,180]. Another challenge was defining the liquid–vapor equilibrium (VLE) of ILs as a function of ΔH_{vap} and Pv while preventing their decomposition at high temperatures. Armstrong et al. [181] studied the vapor phase and ΔH_{vap} of ILs under very high vacuum pressure using line-of-sight mass spectroscopy (LOSMS). It was observed that the vapor phase contains neutral ion pairs and the ΔH_{vap} primarily follows the Coulombic relation between the liquid and vapor phases [181]. molecular modeling was also used to study the vapor phase of ILs [182]. Simulation results show that the vapor phase contains mostly single ion pairs and a significant ion fraction is present in greater masses, which increases as the pressure and temperature rise. Different trials were carried out to determine the ΔH_{vap} of ILs using surface tension, the Knudsen method, temperature-programmed-desorption, microcalorimetry, and molecular dynamics (MD) simulation transpiration [180,183]. Unfortunately, these techniques do not generate consistent ΔH_{vap} for ILs. For example, the calculated values for the ΔH_{vap} for [omim][Tf_2N] ILs were found to be in the range of 150 to 192 kJ/mol [184]. However, as reported by Rebelo et al. [185], credible values for ΔH_{vap} range from 120 to 200 kJ/ mol. Similarly, [OMIM][BF_4] and [BMIM][BF_6] have exhibited an excellent UP_{CO_2} capacity in the range 80.8–99.8% with no more of 5–8% loss [186].

Far-infrared calculations were also used to determine the ΔH_{vap} of imidazolium ILs [187] in the range of 128 to 165 kJ/mol. Conversely, LOSMS was employed to determine the ΔH_{vap} of twelve ILs [188]. The calculations follow a simple theory that is based on the sum-up of the Coulombic interaction impact and the contributions of van der Waals forces between the cation and the anion. Rocha et al. [189] published high-precision data on vapor pressure from nine imidazolium-based ILs. The values were determined using quantitative structural separation phenomenon in ILs corrected with the corresponding thermodynamic properties. Data from high-accuracy vapor pressure for all ILs at 450 K was ~ 0.02 Pa. As the pressure is very low and less than normal experimental conditions, the VOL_{IL} of the ILs is still expected. Though, this negligible VOL_{IL} will not negatively impact their applications as green solvents[190]. Vinyl imidazolium amino acid-ILs (AAILs) based on seven amino acids (L-lysine [L-Lys], L-arginine [L-Arg], L-alanine [L-Ala], glycine [Gly], L-proline [L-Pro], L-histidine [L-Hist], and L-valine [L-Val]) were tested for UP_{CO_2} capacity at temperatures ranging from 283. The UP_{CO_2} capacity was ordered as follows: [VBIm][L-Arg] > [VBIm][L-Lys] > [VBIm][Gly] > [VBIm][L-Ala] > [VBIm][L-Val] > [VBIm][L-Pro] Amongst the studied AAILs [VBIm][L-Arg] showed the maximum UP_{CO_2} capacity due to the availability of more amino groups [191].

6. Functionalized ionic liquids (FUN_{ILs})

Functionalized ionic liquids (FUN_{ILs}), also known as task-specific ILs, are intended to enhance the effectiveness of traditional ILs in a specific application by modifying the constitutive ionic structure. In the last decade (2012–2022) ILs science has witnessed the development of three types of FUN_{ILs} that target the CAP_{CO_2}: cationic-functionalized ILs (CAT-FUN_{ILs}), anionic-functionalized ILs (AN-FUN_{ILs}), and dual-functionalized ILs (CAT/AN-FUN_{ILs}). The goal of tuning such functional groups is to enhance the UP_{CO_2} efficiency by improving the CO_2-ILs connection. Such configurations paved the way for the development of novel ILs that can be used at large scale for CAP_{CO_2} from industrial streams. Recently, a two-dimensional ionic liquid (2D-IL) composed of 2D-ordered mono-ionic IL structures was developed. The 2D-IL demonstrated ultrahigh UP_{CO_2} capacity and a long recyclability life span due to anomalous stepwise melting processes involving localized rotated, out-of-plane flipped, and fully disordered states [52].

As discussed before, the low P_{CO_2} is the most limiting factor for the CAP_{CO_2} from $Post_{com}$ process using ILs. It was reported that the S_{CO_2} in wide varieties of ILs even for the best physically structured is < 5 mol%. Trials on connecting amine chemistry with ILs have significantly improved the efficiency of the CAP_{CO_2}. Thereafter, the tuning and development of such kinds of ILs were exponentially expanded.

6.1. Cationic functionalized ILs (CAT-FUN_{ILs})

The idea of functionalized ILs (FUN_{ILs}) was first presented by Bates et al. [192,193]. The authors grafted an imidazolium cation with main amine fraction and CAT-FUN_{IL} that has the UP_{CO_2} of 2:1. These two studies showed that the stoichiometry of the CAP_{CO_2} was comparable with the maximum theoretical molar limit of CAP_{CO_2} by the traditional amine system. The UP_{CO_2} was reversible suggesting a promising simple regeneration step. The developed CAT-FUN_{IL} was regenerated under vacuum in the temperature range of 80 to 100 °C. Ding et al. [194] include an *in situ* polymerization of confined imidazolium-based poly ILs (IL_{poly}) into the metal–organic framework (MOF) material to produce IL_{poly}-MOF. The developed IL_{poly}-MOF exhibited an excellent CAP_{CO_2} with high UP_{CO_2} capacity. Bernard et al. [30] showed that mixing amine with [BEIM]BF_4 displayed varied UP_{CO_2} capacities depending on the amine type. This study shows that the combination MDEA + [BEIM]BF_4 has a high cycling UP_{CO_2}, is energy efficient, has good regeneration ability, and exhibited low viscosity. Chen et al. [195] developed a framework with guanidine-embedded poly and a sequence of ultramicroporous N-doped carbons IL. Within the polymeric frameworks, the crosslinking agent (MBA) and the IL monomer (1-(4-vinylbenzyl)-tetramethyl guanidinium chloride) were distributed to produce a significant specific surface area of 1606.1 m^2/g, a significant amount of ultra-micropores (<0.7 nm) at 0.4314 cm^3/g, and a significant amount of pyrrolic-N sites. This structure exhibited an excellent UP_{CO_2} capacity of 3.95 mmol/g, and SEL_{CO_2} of 20.4 at 25 °C and 1 bar. Recently, [3-AP][TFA] and [MDEA][TFA] were tested for UP_{CO_2} under different mixing ratios in the range 2:1 to 1:6. Results showed that [3-AP][TFA] achieved $UP_{CO_2,Max}$ of 0.91 mol_{CO2}/mol_{IL} at ratio 1:6, [MDEA][TFA]. The optimum ratio of 1:4 was found to achieve UP_{CO_2} of 0.93 mol_{CO2}/mol_{IL}. The

obtained results suggest that increasing the UP_{CO_2} capacity does not require a high amount of MDEA [196]. Similarly, it was confirmed that mixing MEA and DEA with [Rmim][Tf_2N] exhibited differently UP_{CO_2} Capacity as shown in Fig. 4. The observed UP_{CO_2} of ILs-amine is two order of magnitude higher than IL- DEA [197].

The IL_{poly} with polyurethane structures are being explored as viable CAP_{CO_2} materials. As a result, a variety of anionic ILs_{poly} based on polyurethane was created, and the impact of polyol chemical structure and counter-cations (imidazolium, phosphonium, ammonium, and pyridinium) on UP_{CO_2} at different CO_2/CH_4 ratio was investigated. The PILPC-TBP was shown to be the best poly (ionic liquid) for UP_{CO_2} from a mixture of CO_2 and CH_4. When compared to previously studied poly (ionic liquids), poly (liquid ionic) base polyol (polycarbonate) with phosphonium (PILPC-TBP) displayed greater UP_{CO_2} capacity (21.4 $mgCO_2/g$ at 303.15 K and 0.08 MPa). Sánchez et al. [198] developed dual CAT-AN_{IL} by grafting the CAT_{IL} [bmim] with primary and tertiary amines. The generated CAT were combined with AN_{ILs} [DCA] and [BF_4]. The S_{CO_2} of the developed CAT-AN_{ILs} ([bmim][DCA] and [bmim][BF_4]) did not considerably enhanced. However, grafting the CAT_{IL} [bmim] with AN_{IL} amino group [Ambim] significantly enhanced the CAP_{CO_2} at a temperature of 303 K and pressure 0.1 MPa by a factor of 13 and 14 for the [Ambim][BF_4] and [Ambim][DCA], respectively [198]. Therefore it was suggested that the S_{CO_2} was improved due to the addition of amine groups to the CAT_{IL}. The examined isotherms demonstrate that the connection between CO_2 and FUN_{IL} is due to chemical absorption. Suggesting that CO_2 could be removed from the required stream even at low pressures. The amine-grafted ILs showed better UP_{CO_2} than tertiary-amine-grafted IL [3Amim][BF_4]–CO_2 due to significantly lower S_{CO_2} in the later functionalized IL. This trend was aimed to lower reactivity between tertiary amines and CO_2 [65]. The FUN_{IL} did not exhibit a decreased in UP_{CO_2} capacity after being reproduced at 353 K in vacuum pressure. However, the viscosity issues with CO_2 were noted again after the reaction.

The FUN_{ILs} have been shown to produce promising results in CAP_{CO_2}. However, the problem with these FUN_{ILs} is their high viscosity, which makes scaling up difficult. To address the viscosity issue with amine-FUN_{ILs}, nongrafted room-temperature ionic liquid (NRTIL) amine solutions were suggested by Camper et al. [197]. It is known that most ILs exhibit higher UP_{CO_2} with the increase in operating pressure. Some NTSILs can have significant UP_{CO_2} even at low pressure due to their greater CO_2 reactivity [199]. Therefore a solution compromised of 50 mol% MEA with NRTIL was able to bring the UP_{CO_2} close to 2:1, which is close to the stoichiometry of 1 MEA process [101]. With such a strategy, the viscosity of ILs could be decreased from ~ 20 mPa.s to values similar to the viscosity of aqueous MEA solutions (<3.1 mPa.s). It was reported that the viscosity of NRTIL and 30 wt% MEA solution at 25 °C is 2.2 mPa.s. Yu et al. [200] explained the observed high viscosities using molecular simulation. Results showed that adding an amino group around the imidazolium ring does not affect the anionic arrangement as the anions are uniformly arranged over the $–NH_2$ via strong hydrogen bonds. However, the coefficient of ionic self-diffusion was observed to decrease by folds compared with the non-functionalized counterparts, which increased the viscosity. Similarly, molecular modeling was used by Gutowski and Maginn [201] to clarify the dramatic viscosity increases during the CAP_{CO_2} using amine-grafted ILs. It was concluded that the viscosity increases due to the slow translational and rotational dynamics of amine-grafted ILs in addition to the formation of a strong pervasive hydrogen-bonded network.

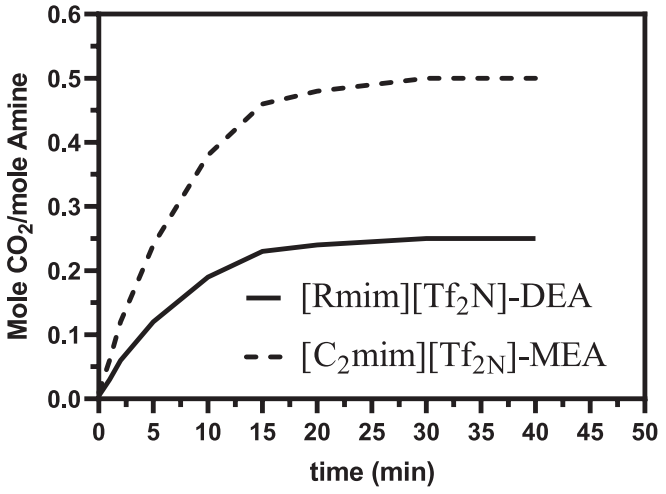

Fig. 4. The UP_{CO_2} in equimolar solutions of [C_2mim][Tf_2N]-MEA and [Rmim][Tf_2N]-DEA. Reprinted with permission from reference [197].

6.2. *Anionic functionalization ILs (AN-FUN_{ILs})*

Although CAT-FUN_{ILS}, such as amine-functionalized cations are effective CAP_{CO_2} process as Pre_{com} conditions, the reaction stoichiometry of 1:2 should be improved to enhance the process efficiency and feasibility. Gurkan et al. [202] showed that the 1:2 stoichiometry in the amine-functionalized cation systems is related to the formation of carbamate during the binding of amine with a cationic group. It was suggested that the stoichiometry ratio could be decreased to 1:1 by attaching an amine group to a chosen anion group. Two amino acid-based ILs, [$P_{666,14}$][Met] and [P_{66614}][Pro] achieved this stoichiometry ratio. Fig. 5 exemplifies the expected isotherms of CAP_{CO_2} via AN-FUN_{ILS} with a stoichiometric ratio of 1:1. The isotherms can be broken down into two distinct components: a sharp increase at low pressure caused by chemical absorption and a slight increase in capacity at higher pressure due to physical absorption. Chemical absorption has the major contribution to the CAP_{CO_2} leading to a stoichiometric ratio of 1:1 as confirmed by FTIR measurements [202]. Still, the amine-grafted ILs are characterized by high enthalpy and viscosity. The enthalpies of the CAP_{CO_2} reactions using [P_{66614}][Pro] and [P_{66614}][Met] were determined at 25 °C to be −80 and −64 kJ/mol, respectively. It was concluded that these values represent the average values of physical (-10 to −20 kJ/mol) and chemical (-85 to −100 kJ/mol) absorptions of traditional amines. In comparison to the cation-functionalized ILs, the viscosity increase by reaction with CO_2 due to the formation a hydrogen-bonded network. Similar trends were observed in different studies [86,203,204]. The CAT-FUN_{IL} ([P_{66614}]) combined with de-protonated anions of amino acids, such as isoleucinate and glycinate exhibited a viscosity increase by 240-fold in comparison to the neat ILs. The increase in viscosity would require more energy to pump the viscous IL at the same time the CAP_{CO_2} will weaken due to the decrease in the diffusion of CO_2 in viscous ILs. Voskian et al. [205] produced AN-FUN_{IL} of ethylenediamine with a good UP_{CO_2} of roughly 0.95 mmol (42 mg_{CO2}/g_{IL}). The viscosity of the AN-FUN_{IL} was rather high, which most likely imposed kinetic and gas contacting constraints on the cell. Shahrom et al.[206] examined the CAP_{CO_2} of eight amino acids-LIs (arginine [Arg], lysine [Lys], histidine [Hist], taurine [Tau], proline [Pro], serine [Ser], alanine [Ala], and glycine [Gly]). The [Lys] had the greatest UP_{CO_2} within the wide family tested, with 15.7 wt%. In terms of molar adsorption, [VBTMA][Arg] had the maximum UP_{CO_2} capacity of 0.83 mol/mol, which rose to 1.14 mol/mol following polymerization. The IL regeneration process was observed to enhance by at higher pressure and lower temperature, achieving maximum CO_2 desorption at 80 °C. It was also reported that this materials has high recyclability maintaining 86 % of UP_{CO_2} capacity on the fifth cycle. Recently, a new imidazolium-based TIL (TCMI-IL) was synthesized using three amine-based chains [207]. The physical and chemical characteristics of a new tricationic ILs were determined using a simple and successful production process. The effect of absorption temperature and IL content was studied at various equilibrium pressures ranging from 90 to 240 kPa. The tricationic IL exhibited an excellent UP_{CO_2} and great structural flexibility.

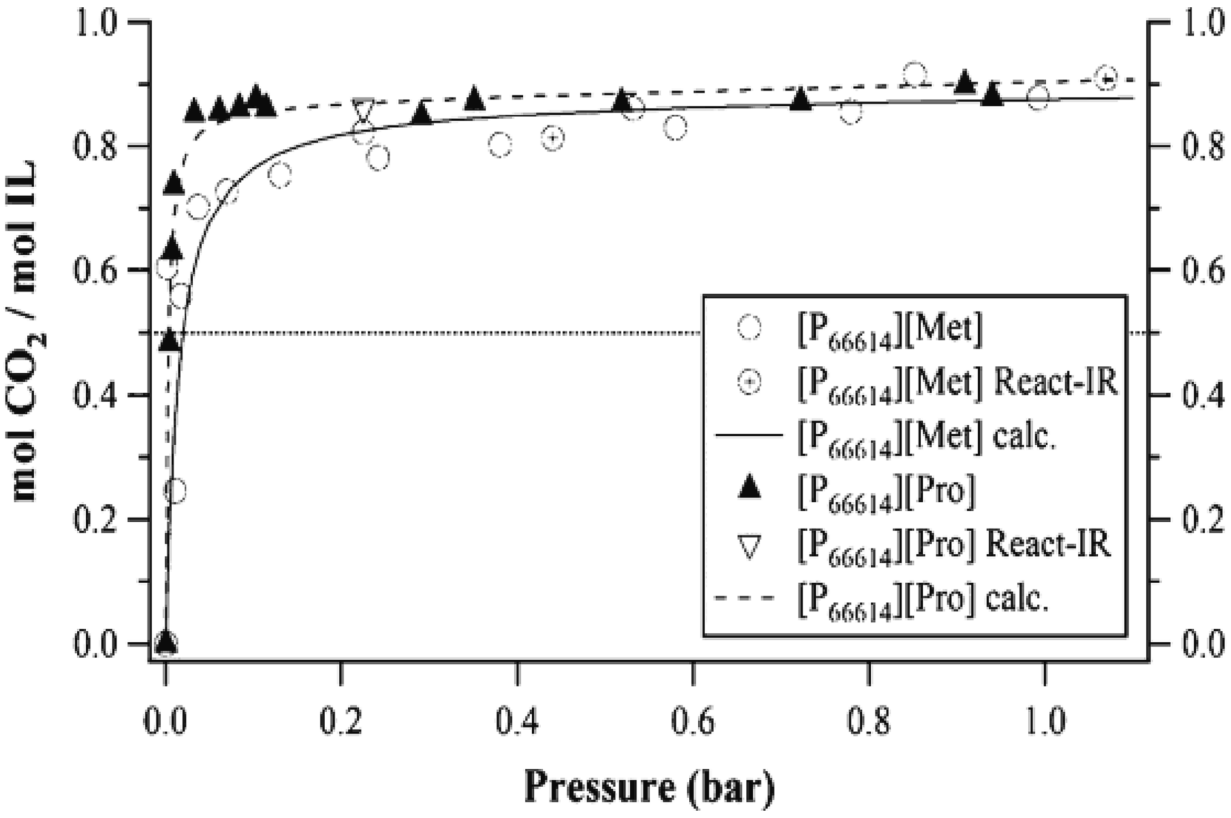

Fig. 5. The UP_{CO_2} using AN-FUN_{ILS} [P_{66614}][Pro] and [P_{66614}][Met] at 22°C. Printed with permission from [101].

Cyano-based AN-FUN_{ILS} composed of 1-hexyl-3-methylimidazolium tetracyanoborate ([hmim][TCB]) was used by Amiri et al. [208] to UP_{CO_2} from gas stream containing CH_4 and CO_2. The developed [hmim][TCB] exhibited high UP_{CO_2} capacity and showed low viscosity compared to the organic ILs (DEPG-Selexol). The developed [hmim][TCB] showed an excellent tendency to UP_{CO_2} from a feed gas stream containing 20 to 40 mol % CO_2 compared with DEPG-Selexol. This excellent UP_{CO_2} *the* tendency was maintained even at a lower percentage of CO_2 down to 5 mol%. The proposed [hmim][TCB] was regenerated using swing pressure and temperature processes. Combining AN-FUN_{ILS} with anions, such as acetate was also reported as a successful material for CAP_{CO_2}. Wasewar et al. [209] examined the efficiency of the combination of AN-FUN_{ILS} with acetate ([bmim][acetate]) diluted to 14 wt% in solution for CAP_{CO_2}. The 14 wt% AN-FUN_{ILS} exhibited an excellent UP_{CO_2} capacity, with volumetric UP_{CO_2} capacity of ~ 25 m^3/m^3. This value is higher than physical ILs (~ 3 m^3/m^3), however, it is still<30 wt % aqueous MEA in the solution (~ 65 m^3/m^3). Maginn et al. [210] showed that the UP_{CO_2} by [bmim][acetate] system is due to proton removal from the imidazolium ring C_2-position by the effect of acetate anion, which resulted in acetic acid. However, the study of Shiflett et al. [211] found that the method of acetic acid production presented by Maginn et al. [210] is not very favorable. Other experimental tests identified the production of acetic acid in the reactor [211]. The authors categorized the CO_2^+[bmim][acetate] system phase performance as highly uncommon with powerful intermolecular interactions and complicated reactions. Recently, novel hybrid materials consisting of ILs supported on low-cost renewable resources (e.g., the microporous structure of carbonized agave bagasse fibers) were developed to increase the UP_{CO_2} capacity. As presented before, the IL 1-butyl-3-methylimidazolium acetate[212] has an excellent UP_{CO_2} with strong CO_2 affinity. The UP_{CO_2} capacity after adding this IL to carbonized fibers (CF), acid-washed carbonized fibers (CFw), and impregnated carbonized fibers was assessed using different mass ratios of CO_2. The combination of CF-IL at a mass ratio of 1:103 increased the UP_{CO_2} from 0.77 for the IL to 1.29 $mmol_{CO2}/g_{IL}$ for CF-IL. The tests that was carried out for 50 min showed that the new combination increased the UP_{CO_2} rate from 0.012 to 0.02 $mmol_{CO2}$/min.g, suggesting an excellent tendency for CAP_{CO_2}.

Wang et al.[213] grafted the superbase-derived protic ionic liquids (S-DP_{ILs}) denoted as (MTBD) with six powerless proton donors including different partially fluorinated alcohols (TFE, TFPA, HFPD, phenol, pyrrolidone, and imidazole). All the combinations demonstrated great properties for CAP_{CO_2}. For instance, the [$MTBDH^+$]/[TFE^-] exhibited fast UP_{CO_2}, *the* low viscosity of 8.63 cP@ 23 °C and high UP_{CO_2} capacity of 1.13 $mol_{CO2}/mol_{S\text{-}DPILs}$. In addition, it was reported a very small capacity loss of these S-DP_{ILs} after numerous UP_{CO_2} cycles. Regeneration of these S-DP_{ILs} was carried out using nitrogen aeration at 80 °C. Another form of hybrid material of polyamine-based protic ionic liquid (PIL) was produced by impregnating SBA-15 with tetraethylenepentammonium nitrate [TEPA][NO_3] and mesoporous silica [214]. This novel hybrid adsorbent exhibited UP_{CO_2} rate of 147 × 10^{-3} mmol/g.s, which is threefold higher than existing IL-functionalized and amine-modified support systems. Furthermore, the UP_{CO_2} capacity can be increased to 2.15 mmol/g by increasing the temperature to 333 K and reducing the pressure to 0.15 bar, indicating outstanding performance under low P_{CO_2}. Again, regeneration of this compound was carried out using nitrogen aeration at 373 K restoring about 90% of the initial UP_{CO_2} capacity. Table 4 presents the CO_2 solubility for some functionalized ILs.

7. Reversible ionic liquids

Heldebrant et al. [216] and Latini et al. [217] presented innovative technology for CAP_{CO_2} with reversible ionic liquids (RILs). It was demonstrated how RILs can be produced by exposing a non-ionic liquid (NIL), such as an amine base or alcohol to CO_2 to create IL salt. Then, it can be returned to its non-ionic first condition by reacting with nitrogen or another inert gas [218]. This type of solvent is denoted as a convertible solvent as its polarity can be changed during the reaction with CO_2. Heldebrant et al. [216] examined the UP_{CO_2} using DBU in the

Table 4
The S_{CO_2} in a number of functionalized ILs.

Iionic Liquid	Functionality	Temp. (K)	Pressure (bar)	$S_{CO_2,max}$ (CO_2/mol_{IL})	Ref.
Bmim [Tau]	NH_2-Anion	–	–	0.44	[215]
Bmim [Gly]	NH_2-Anion	–	–	0.4	[215]
APMim [DCA]	NH_2-Anion	303	0–10	0.29	[56]
APMim [BF_4]	NH_2-Cation	303	0–10	0.33	[203]
APMim [NTF_2]	NH_2-Cation	303	0–10	0.26	[203]
AEMPyrr [BF4]	NH_2-Cation	–	–	0.27	[56]
MeImNet2 [BF4]	NH_2-Cation	–	–	0.25	[56]
[P_{66614}] [Pro]	NH_2-Cation	–	–	0.56	[215]
[P_{66614}] [Gly]	NH_2-Cation	300	5.5	0.574	[203]
[P_{66614}] [Sar]	NH_2-Anion	–	1000	0.523	[203]
[P_{66614}] [Met]	NH_2-Anion	–	18	0.568	[203]

presence or absence of water. The results indicated that the DBU in the presence of water produce [$DBUH^+$][HCO_3^-] to promote UP_{CO_2}. However, the UP_{CO_2} efficiency of such IL in the absence of water is low and therefore its suitability as CAP_{CO_2} is limited. Comparable chemistry was obsrrved for a mixture of guanidine/alcohol during the UP_{CO_2} from gas stream [54]. However, in such reaction the product is carbonate salt. The advantage of this combination is that it can be reversible to non-ionic conditions by bubbling nitrogen or applying moderate heat with the reactor.

RILs produced from organic alcohols and amidine/guanidine were also proposed as an efficient method for UP_{CO_2} [219]. Their production required less than half of the energy required in the preparation of MEA solution. Therefore, has application that is more practical. It was demonstrated how CO_2 is reversibly and chemically binding to the RIL, which creates a liquid alkyl carbonate. It was highlighted that the free binding energy of CO_2 to this RIL is very small and related to the selected base (~ − 9 kJ/mol for DBU and 2 kJ/mol for1,1,3,3-tetramethylguanidine). Moreover, the formation of this RIL as liquid eliminate the need for adding solvent. The UP_{CO_2} efficiency of this RILs was>19 wt%, which is comparable to MEA. The UP_{CO_2} and SEL_{CO_2} of this RILs did not exhibit any decrease after five cycles even with the presence of N_2 [219]. The reaction enthalpy of CO_2 in Barton's base is also similar to MEA, whereas it was more significant for the DBU/alcohol and TMG/alcohol mixtures. However, in the presence of water unwanted bicarbonates were produced, which is particularly concerning because flue gas can include significant quantities of water.

A single-component RIL produced from siloxylated amines for effective UP_{CO_2} though the carbamate salt [220]. Other four silylated amines combined with RILs were examined for UP_{CO_2}. It was observed that the silyl amines showed excellent UP_{CO_2} capacity and they were stable in the presence of water, whereas the siloxylated amines showed high degradation ability. The mechanism of UP_{CO_2} using these RILs has mixed physico-chemical properties. The UP_{CO_2} capacity at 35 °C and 62.5 bar was found in the range of 13–20 mol CO_2/kg_{amine}. The added flexibility of similar RIL is presented by Jessop et al. [221]. Biobased ILs (Bio-ILs) produced from choline/amino acids and ionic metathesis were proposed by Latini et al. [222]. The UP_{CO_2} of such bio-ILs were tested experimentally. Simethyl sulfoxide (DMSO) was used as a solvent to avoid the viscosity issues. The RIL-DMSO solutions with varying IL concentrations were tested for UP_{CO_2} under real-world industrial conditions. Tests were focused on UP_{CO_2} capacity, RILs recyclability and the potential biological and toxicological side effects. Tests demonstrated the non-toxicity and good biocompatibility of these bio- ILs with an excellent UP_{CO_2} capacity > 0.5 mol CO_2/mol_{IL}) under mild to higher conditions.

8. The efficiency of IL against commercial solvents for CAP_{CO_2}

The UP_{CO_2} using ILs relies on their behavior and interaction with solvents used in the process. Therefore, when comparing the performance of ILs against commercial solvents for UP_{CO_2}, properties such as selectivity, viscosity, absorption capacity, stability, and cost should be considered. Table 5 summarizes the performance of ILs for UP_{CO_2} against six commercially used solvents. The Selexol, Fluor, Purisol, and Rectisol were used alone and based on physical UP_{CO_2} whereas the Sulfinol and sulfolane solvents were mixed with MDEA and DIPA, respectively. In the econamine method, Fluor is mixed with at least 30 wt% MEA to achieve excellent UP_{CO_2} via chemical absorption [223]. It was reported that these solvents are used in the industry for the natural gas sweetening method. The selection of CAP_{CO_2} solvent would be based on the operational conditions, gas partial pressure, products and contaminants characteristics [224]. The ILs solvents outlined in Table 5 exhibit physical UP_{CO_2}. Reports on the cost of using different ILs as CAP_{CO_2} process under large scale is higher than conventional solvents by a factor of 10 to 20 [101,225]. As such, the successful use of ILs is dependent on other IL properties. As discussed before, the viscosity of ILs, in general, is higher than commercial solvents (DIPA and MEA) and does not considered as an advantage toward using ILs for UP_{CO_2}. However, considering the fact that ILs are always applied in a diluted form that are not significantly greater than water viscosity. The viscosity issue is no longer a problem. An essential property of ILs that support their use for UP_{CO_2} is their low vapor pressure compared to currently applied solvents. Most of the proposed ILs have vapor pressure and in-solution lower viscosity comparable with the successfully used Selexol method.

Another property that supports the use of ILs for UP_{CO_2} is their low volatility (VOL_{ILs}). The MEA, which is considered the most commonly used process for UP_{CO_2} suffer from high volatility and high thermal degradation, which significantly affect the efficiency and the cost of the UP_{CO_2} process [227,228]. Rochelle et al. [229,230] reported an overall loss of 80 to 540 g/ton of MEA at the stripper in the temperature range of 110 to 30 °C. Losses result in solvent replacement costs ranging from $0.19 to $2.31/ton [229,230]. Hospital-Benito et al. [231] showed using Aspen Plus simulation that IL can be a cost-effective solution for UP_{CO_2} from Pre_{com}. The study confirmed that the used the IL [P2228][CNPyr] can be regenerated at 1 bar. The cost of UP_{CO_2} was determined to $ 40/t_{CO2}. Regenerating the IL at 1 bar and at elevated temperatures would match the flue gas operating conditions and allow avoiding the high equipment costs associated with vacuum regeneration processes. In addition, this would decrease the associated utilities cost and minimize the heat transfer gap between processes. When just direct costs were taken into account, the minimal cost reached was $ 64.1/t_{CO2}, based on an IL scaled up price of $ 50/kg, but it might possibly be further less than $ 40/t_{CO2} next generation solvents.

Considering this fact, the low volatility and thermal stability of ILs under different operational conditions would suggest their economical use for UP_{CO_2}. In fact, combining ILs and MEA in some studies aimed to solve the volatility and thermal stability of MEA. Akinola et al. [232] showed that mixing [bpy][BF_4] with MEA could reduce the costs of reboiler duty and CAP_{CO_2} by around 15% and 7.44%, respectively. Another advantage of using the ILs for UP_{CO_2} is their low corrosivity to carbon steel compared to the MEA process. It has also been observed that some ILs are anti-corrosion agents [233]. There is little research work on the corrosion and degradation performance of ILs, and more research is needed. Yet, when combined with copper alloys, particularly at higher temperatures, several of the regularly used ILs can be corrosive [234,235].

The previous analysis of the cost of the ILs process against the per-

Table 5
Comparison between ILs and commercial solvents used in $CAP_{CO_2}{}^{(*)}$.

	Flour solvent	Selexol	Rectisol	Purisol	Sulfinol	Econamine FG	Ionic Liquids
Absorption type	Physical	Physical	Physical	Physical	Physical/ Chemical	Chemical	Physical
Viscosity (mPa.s)	3	5.8	0.6	1.65	186	18.98	20–1000
Density (kg/m^3)	1195	1030	785	1027	1004–1261	1017	800–1500
Molar mass (g/mol)	102	280	32	99	120.1–133.1	61.09	200–750
Vapor pressure (mmHg)	0.085	0.00073	125	0.4	0.02–0.035	0.36	0.000001
Freezing point (℃)	−48	−28	−92	−24	26–44	10.5	−140 to180
Boiling point (℃)	240	275	65	202	249–285	171	> 250
Maximum Temp (℃)	65	175	65	202	150	150	Depend on stability
Maximum Pressure	high	high	high	high	Low	Low	high
CO_2 solubility (m^3/m^3)	3.4	3.63	14.4	3.57	30–40	50–85	> 2.51
CO_2/CH_4 *SEL*	26	15	20	14	NA	NA	8–35
Δ_{vap}H (KJ/mol CO_2)	117	50	83	50	NA	NA	30–100
H_2S/CO_2 *SEL*	3.3	8.8	7	10.2	1–2	1–2	2–10
CO_2/H_2 *SEL*	126	77	185	178	NA	NA	50–150
H_2O miscibility	Partial	Yes	Yes	Yes	Yes	Yes	Variable
CO_2/N_2 *SEL*	60.2	76.16	35.27	54.5	57.4–66.8	49.8	>120

Data were taken from references [101,114,140,144,146,154,161,163,226].

formance suggests that this technology is attractive. In addition, the tunability of ILs could be used to develop and design cost-effect and thermally stable ILs with high UP_{CO_2} capacity and selectivity. These ILs could be used alone or combined with traditional solvents. The ILs could also be designed to work within a range of physical (i.e., traditional) solvents. For instance, at $Post_{com}$ conditions when P_{CO_2} is extremely low, the high-energy efficiency amine grafted IL with reaction stoichiometry can be an effective method for UP_{CO_2} compared to the Sulfinol or MEA method alone. In contrast, processes with high P_{CO_2} standalone IL could be employed (see Table 1) due to its high S_{CO_2} under such conditions. The price vs performance of ILs could be enhanced by using supported ionic liquid membranes (SILMs) and is presented in the next section.

9. Supported ionic liquid membranes (SILMs)

Recent research has focused on SILMs as CAP_{CO_2} technology. The SILMs consist of IL attached to the pores of polymeric and/or inorganic membranes by capillary forces [53]. The SILMs are considered heterogeneous UP_{CO_2} technology because they have the two phases. The membrane solid phase and the attached ILs as liquid phase. Different solute particles are used to dissolve or diffuse ILs on the surface of membranes [236]. As one of the major draw back of the traditional ILs is the material loss. The SILMs with stable structure have less solvent loss, more stabilized liquid phase and exhibit lower evaporation [237,238]. Therefore the SILMs technology advantage of ILs distinctive characteristics such as low VOL_{IL} and high thermal and chemical stability [239]. The use of SILMs technique for UP_{CO_2} has been examined in numerous studies [240-243]. Scovazzo et al. [240] showed that the SILMs developed at room temperature outperformed standard polymers for UP_{CO_2} from streams that contain CO_2, CH_4, and N_2 even at low P_{CO_2}. Yoo et al. [241] tested the UP_{CO_2} of three CAT_{ILs} containing 1-n-hexyl-3-methylimidazolium ([hmim]) supported on stable polysulfone asymmetric support ([PF_6] or [PF_4]). The combinations [hmim][BF_4] and [hmim][BF_6] increased the UP_{CO_2} separation factor from a mixture of CO_2 and CH_4 to 26. Iarikov et al. [242] developed SILMs using 1-amino pyridinium iodide dissolved in 1B4MPTFB. The as-prepared SILMs displayed an excellent CO_2 permeance in the order of 5×10^{-10} to 5×10^{-9} mol/m^2.s.Pa combined with very high S_{CO_2} of 5–30. Bara et al. [244] and Noble and Gin [245] assessed the use of SILMs for gas separation using a Robeson plot combined with the data from polymeric membranes. It was confirmed that the Robeson plot could be used to identify the trade-off between permeability and SEL_{CO_2} form a mixture of CO_2 and N_2. Comparable results were noticed in other studies [246,247]. In all the previous studies, it was concluded that that the use of polymeric membranes offers an excellent opportunity to design SILMs with a higher SEL_{CO_2} and permeability than conventional polymeric membranes. The mechanism of transportation of gas is based diffusion controlled mass transfer [246]. The diffusion coefficient (D_i) is lineally proportional to the product of the solubility and inversely proportional to the ideal gas permeability (P_i) as per Eq. (3):

$$D_i = \frac{S_i}{P_i} \tag{3}$$

There are a number of relationships that can help to estimate the diffusivities of gas [178,248] and solubilities [129,153] in ILs. Scovazzo's [249] focused on the development of the SILM area and outlined higher limits and standards for future use. The UP_{CO_2} capacity was linked to the molar volume and the *SEL* of IL to the combined gases, such as CO_2/CH_4 and CO_2/N_2 as well as the reliance of the IL viscosity on CO_2 permeability. Camper et al. [250] identified the common correlation that is expected to improve the *SEL* by reducing the IL molar volume for the combined gas CO_2/N_2 and CO_2/CH_4.

Different works described the SEL_{CO_2} in SILMs for a mixture of CO_2/N_2 [236,251-253]. Scovazzo [236] showed that the CO_2 permeability and SEL_{CO_2} from CO_2/N_2 mixture range between 3.50×10^4 –1.0×10^6 cm^3 (STP) cm/cm^2.s.cmHg, and 15–61, respectively. Similarly, Bara et al. [251] evaluated the $S_{CO_2}, S_{N_2}, S_{O_2}, S_{CH_4}$ in fluoroalkyl-grafted imidazolium-based SILMs. Reported CO_2 permeability ranged from 210 to 320, whereas the S_{CO_2} in CO_2/N_2 and CO_2/CH_4 mixtures were in the range 16–27 and 13–19, respectively. Neves et al. [252] showed that the IBIL has a S_{CO_2} in the range of 20–32 and 98–200 for mixtures of CO_2 and N_2 or CO_2 and CH_4, respectively. The SEL_{CO_2} from gas mixtures of CO_2 and N_2, CO_2 and H_2, and CO_2 and CH_4 treated with SILMs that contain several types of ILs were in the range of 10–52, 5–13, and 5–23, respectively [253]. For example, [emim][Tf_2N] and [emim][BF_4] based SILMs achieved SEL_{CO_2} of 21.2 and 27 for a gas mixtures of CO_2 and N_2 and CO_2/CH_4, respectively [240]. In all the previous works, it was concluded that the reported SEL_{CO_2} was nearly identical to the ideal selectivity for comparable combined gases.

Myers et al. [254] tested the UP_{CO_2} from a mixture of CO_2 and H_2 using amine-grafted IL in a cross-linked Nylon 66 support using. The SEL_{CO_2} was 15 while the CO_2 permeability ranged from $1.0x10^4$ to 1.0×10^7 cm^3 (STP) cm/cm^2.s.cm.Hg. Scovazzo et al. [246] concluded that the S_{CO_2} the SEL_{CO_2} in SILMs is very high, while diffusion verifies the *SEL* in polymers. Further information on SILMs is presented in the outstanding reviews by Scovazzo [246] and Lazano et al. [255].

A new class of benzimidazole-based hyper-cross-linked poly ionic liquids (HPILs) with high specific surface area in the range 485–780 m^2/g, abundant micro/mesoporosity, and numerous ionic active sites was developed by Sang et al.[256]. The HPILs demonstrated significant UP_{CO_2} capacity (9–143 mg/g) and SEL_{CO_2} (23–46) under mild conditions

(273 K and 1.0 bar). Surprisingly, the HPILs-Cl-2 exhibited outstanding catalytic activity for CO_2 cycloaddition, effectively converting 99 % of propylene oxide to cyclic carbonates under mild conditions (70 °C, 0.1 MPa CO_2, 9 h). Huang et al [257] tested the UP_{CO_2} by a new SILM prepared by impregnated AAIL and [APMIM][Lys] into a mesoporous silica pore-expanded SBA-15 (PE-SBA-15) and a commercial PMMA substrate. The UP_{CO_2} capacity of the developed SILM was an excellent tendency that depends on the AAIL loading and dispersion on the surface of the supports [258]. The isosteric enthalpy of the UP_{CO_2} was computed using Freundlich model and the Clausius-Clapeyron equation. It was concluded that composite prepared with 50 wt% [APMIM][Lys]-based PMMA has the largest UP_{CO_2} capacity, quick adsorption kinetics, and improved CO_2 chemisorption. A news SILM prepared from nitrogen-rich porous organic polymers (POPs) showed promising catalytic activity for CO_2 cycloaddition as well as UP_{CO_2}. However, their use in the additive-free catalytic conversion of CO_2 into cyclic carbonates remains a challenge. Another SILM was prepared from POPs of nitrogen-rich click-based mixed with imidazolium-based (I-BILs) [259]. The connection between I-BILs and POPs enhanced the structure porosity, CO_2 adsorption/desorption, SEL_{CO_2}, and catalytic activity for chemical transformation. The improved catalytic activity was correlated to the porous characteristics of CPP that work synergistically to catalyze the reaction. Ren et al. [260] showed that the supported IL ([N1111][Gly]) impregnated with PMMA produced a composite MMA-[N1111][Gly] with an excellent UP_{CO_2} capacity. The MMA-[N1111][Gly] achieved equilibrium after 60 min marking a UP_{CO_2} capacity of 2.14 mmol/g at 35 °C. it was highlighted that the UP_{CO_2} rate of PMMA-[N1111][Gly] can be shorten to 4 min if the temperature increased to 75 °C. Cao et al. [261] developed porous poly IL crystallines with various and customizable framework moieties. The as-prepared porous poly ILs demonstrate significant UP_{CO_2} capacity with excellent SEL_{CO_2} from mixtures of CO_2, N_2, and CH_4. Using the advantage of the bifunctionality of ILs for UP_{CO_2} and as catalysts to convert CO_2 to other products was discussed by Hernández et al. [262]. It was concluded that IL cloud be design to act a valuable CCU systems or catalysts for the conversion of CO_2 to other products. Sang et al. [263] resented a bifunctional ionic hyper-cross-linked polymers that can achieve UP_{CO_2} capacity134 mg/g at 273 K, and 1.0 bar), moderate isotopic adsorption heat of 28–38 kJ/mol), and excellent $_{CO2}$ cycloaddition ability.

Huang et al. [264] prepared a new SILM compromised of amino-functionalized ionic liquid (AFIL) mixed with [TETAH][Lys] and dissolved in an ethanol–water solvent. Tests on this SILM showed that the [TETAH][Lys] solution separated into two phases after UP_{CO_2} process. The volume of the CO_2-rich phase was approximately one-third of the total volume, suggesting that only one-third of the solution required regeneration. Therefore, the required energy was reduced by a factor of 3. The UP_{CO_2} capacity reached approximately 93 % of the maximum loading capacity and the viscosity did not exceed 27.95 mPa.s. In addition, the [TETAH][Lys] was able to maintain the UP_{CO_2} capacity of 91% after 5 cycles. Another dual-functionalized ionic liquid ([DETAH][T_z]) dissolved into 1-propanol-water solvent was prepared and used for CAP_{CO_2} [265]. The [DETAH][T_z] is characterized by low viscosity (2.57 mPa.s) and an easy regeneration procedure, achieving 96% of the total UP_{CO_2} capacity (1.713 mol/mol), while using only 44% of the total volume. The ([DETAH][T_z] maintained 90% of its UP_{CO_2} capacity after five cycles. The high UP_{CO_2} was attributed to the presence of amine functional groups and the ability of $[T_z]^-$ to undergo an equimolar reaction with CO_2. The presence of [T_z]-H group ensured the facile regeneration efficiency by enhancing the hydrolysis of $RNCOO^-$ to form HCO^{-3} /CO_3^{-2} and propyl carbonate. The SILMs also showed interesting applications in syngas treatment. Wang et al. [266] use a room-temperature technique to remove sour gas from syngas using IL as a physical solvent. It was highlighted that ILs, such as [bmim] [Tf_2N] could be used effectively for the simultaneous removal of H_2S and CO_2 by 97.6 and 95.3%, respectively. Another form of SILMs used for UP_{CO_2} was produced from combining hollow fiber membranes with ILs. Qazi et al. [267] combined the IL ([emim][$EtSO_4$]) with hollow fiber membrane contactors and used it for UP_{CO_2} from combustion flue gas. The UP_{CO_2} tests were performed in a counter-current arrangement. Results showed an excellent UP_{CO_2} removal efficiency. A gas flow rate of 100 mL/min showed an overall mass transfer coefficient and the CO_2 flux of 3.99×10^{-5} m/s and 6.1×10^{-5} mol/m^2.s, respectively. The study showed that the membrane characteristics (wetting, porosity, tortuosity, module length, fiber inner diameter) as well as gas flow rates have direct effect on the UP_{CO_2} effeciency. The UP_{CO_2} is improved by increasing module length and decreasing fiber inner diameter. Rostami et al. [268] investigated the impact of ([Bmim][BF_4]) on UP_{CO_2} utilizing polypropylene hollow fiber membrane contactors. The impacts of several parameters, such as IL concentration, liquid and gas flow rates, and flow direction were studied. The UP_{CO_2} capacity was increased in co-current and counter-current flows by 20 and 15%, respectively, by adding 25 wt % of IL to the solution compared to pure water.

Very recently, the UP_{CO_2} capacity and SEL_{CO_2} under $Post_{com}$ condition was improved using two task-specific ionic liquids (TSILs). The first TSIL consists of [EMIM][glycine (Gly)] and the second one contains [EMIM][alanine (Ala)] encapsulated within the framework of Zeolite imidazolate framework-8 (ZIF-8) [269]. Both TSIL@ZIF-8 resulted in a substantial increase in UP_{CO_2} at a pressures < 1.0 bar. The UP_{CO_2} was larger than pure ZIF-8 at the same. The TSIL@ZIF-8 with only 30 wt% of [Emim][Gly] had a UP_{CO_2} the capacity of 0.76 mmol/g-solid at 0.1 bar and 0.88 mmol/g-solid at 0.2 bar and 303 K. Under all the tested pressures, the TSIL@ZIF-8 demonstrated higher SEL_{CO_2} compared to pure ZIF-8. The impact of encapsulating ILs within the pores of ZIF-8 on UP_{CO_2} was investigated by Thomas et al. [270,271]. The cationic [BMIM] + was coupled with different anionic IL and tested for UP_{CO_2}. Nitrogen-containing anions showed very low UP_{CO_2}, while Fluorinated hydrophobic anions (e.g., [BF_4], [PF_6], and [Tf_2N]) showed an excellent UP_{CO_2} and SEL_{CO_2}. A further examination of the findings reveals that the SEL_{CO_2} of these composite materials is dependent on the anionic part of ILs. Recently, Ribeiro et al. [231] showed that ILs combined with biomass can generate nitrogen-doped (N-doped) porous carbons that can effectively use for UP_{CO_2} or as and catalysts for conversion reactions of the same gas. Similar conclusions were reported by Yu et al. [272].

Garip and Gizli [273] used amine-based silica aerogels to create an adsorption-based technique for UP_{CO_2} from $Post_{com}$ flue gases. The silica-based aerogels were prepared in a single-step sol–gel process using tetraethyl orthosilicate (TEOS) as silica precursor and (APTES) as an amine source. The developed amine-containing IL exhibited excellent SEL_{CO_2}, high S_{CO_2} and low viscosity [274]. Amine-containing IL ([EMIM][TFSI]) was also utilized as a sole agent to improve the UP_{CO_2} capabilities of the generated aerogels. Among the produced aerogels, the $TA_{0.24}IL_{0.28}$ demonstrated excellent UP_{CO_2} behavior, with a capacity of 243.32 mg CO_2/g (5.53 mmol/g).

10. Biodegradability and toxicity of ILs

The ILs are characterized by their low vapor pressure, non-flammability, and stability at high temperatures. However, important issues in green chemistry and sustainability, such as biodegradability (*BioDeg*) and toxicity (*Tox.*) have gone unnoticed. The *BioDeg.* and *Tox.* are essential factors to be determined before the application of any material in industrial applications [275]. It was highlighted in different studies that the biggest obstacle to commercializing IL is the unknown environmental impact [276]. For instance, in the large-scale application of ILs nonbiodegradable or low-biodegradable ILs may present a problem [277,278]. Given that in these applications, ILs might come into contact with waterways through effluent streams, which could affect the local ecosystem. As such, this section explores possible IL threats to humans and the environment within a few specific applications, as well as data that may be applicable to creating safer ILs.

10.1. Biodegradability (BioDeg.) of ionic liquids

The *BioDeg.* of ILs is influenced by their structure, application conditions as well as effluent discharge point [36,55]. The initial stage of marketing a new chemical frequently starts with the molecule design, where the standards of secure design should be applied to ensure safe application. Within this process, the safety data sheet, which includes information, such as the chemical and physical properties, environmental health & hazards; protective measures; and safety are presented. Importantly, the *BioDeg.*of ILs is linked to its molecular structure (anions, cations, and functional groups). Hence, the *BioDeg.* is commonly measured and correlated to the molecular structure. The *BioDeg.*of different chemicals was connected to the forum developed following the guidelines of the Economic Cooperation and Development Organization (OECD) [279]. The OECD is a unique forum in which the governments of 37 democracies with market-based economies collaborate to develop policy standards to promote long-term economic growth. Several techniques conform to OECD rules, including the CO_2 headspace test (ISO 14593), modified sturm test (OECD 301B), die-away test (OECD 301 A), closed bottle test (OECD 301 D), OECD 309, and ASTM D 5988 test. Each technique has a separate concept in which dissolved organic carbon (DOC), CO_2 production, and O_2 uptake should be examined as measures the *BioDeg.*. The suitability of the *BioDeg.*test is determined by the physical properties of the IL. Different authors have outlined the possible procedures to measure the biodegradability of the ILs [278,280,281]. Gathergood et al. [282] and Garcia et al. [283] were the first to describe the weak *BioDeg.* of imidazolium ILs. The closed bottle of [bmim][X] ILs, where X = Br, BF_4, PF_6, TF_2N, DCA, and octyl sulphate showed that the *BioDeg.* of [bmim][X] ILs is very low (<5%) compared with octyl sulphate IL, which exhibited moderate biodegradability of 25%. As such, these ILs cannot be classified as "biodegradable." or green. It was also confirmed that the minimal *BioDeg.* of 60% is required to denote the IL as green in a typical 28-day test time [283,284]. Gathergood et al. [282] used instructions presented by Boethling et el. [285] to enhance the *BioDeg.* of the aforementioned ILs. The requirements must be followed as a general guideline, however, they could also serve as requirements for developing biodegradable ILs. The imidazolium cation's alkyl side chain was modified by adding an ester or an amide group to increase the ILs *BioDeg.* [286]. It was observed that the *BioDeg.* improved by increasing the length of the ester alkyl-chain of the grafted cation. Adding methyl group at the C_2^- location of the imidazolium ring had insignificantly enhanced the *BioDeg.* in comparison to the C^{2-} unreplaced ILs [286]. Conversely, the *BioDeg.* of the ester functionalized ILs was greater than the nongrafted ILs. The attachment of [mim-ester] cation and [octyl sulfate] anion achieved a *BioDeg.* > 60%. Therefore, it was concluded that the ester grafted imidazolium cations with an [octyl sulfate] anion are biodegradable ILs [284,287].

Morrissey et al. [288] estimated the *BioDeg.* of a large amount of imidazolium-based ILs using the CO_2 headspace test. The tested ILs include ester and ether groups in their alkyl part chain. The ILs with Ester groups were biodegradable, whereas ILs containing ether groups showed very low *BioDeg.*. Similarly, Harjani et al. [289] assessed the *BioDeg.* of ester functionalized pyridinium ILs cation combined with multiple anions, including bis(trifluoromethyl sulfonyl)imide, octyl sulfate, Br, PF_6, and iodide using the CO_2 headspace test. The Pyridinium ILs carrying an ester side chain part exhibited high *BioDeg,* while pyridinium ILs with alkyl side chains without ester functionalization were not *BioDeg.*. it was concluded that the impact of the anion on *BioDeg.* is not significant [278,289,290].

Ford et al. [291] analyzed the *BioDeg.* of pyridinium and thiazolium ILs comprised of multiple functionalities, including hydroxyethyl side chain, methyl or ethyl ether side chain, acetal, and carbamate. It was observed that the Pyridinium ILs that include the hydroxyethyl functionality exhibited high *BioDeg.* In contrast, thiazolium ILs that include hydroxyethyl functionality, acetal, ether, or carbamate exhibited low *BioDeg.* Additionally, phosphonium and ammonium ILs as well as octyl sulphate anion showed low *BioDeg.* [292].

10.2. Toxicity (Tox.) of ionic liquids

Toxicologic research is crucial for understanding the influence of ILs on humans and the environment. The *Tox.* of ILs is assessed based on standard methods, such as ISO, ASTM, or OECD. A testing model, such as microorganisms is exposed to the IL and its reaction determines the *Tox.*, which is commonly represented as an IC50, LC50, or EC50 value. Essential data on the *Tox.* of ILs have been presented in several reviews [293-296], in which it is important to highlight the *Tox.* tendencies concerning IL cations, anions, and functional groups. The cation is considered crucial for verifying the IL *Tox.* [297,298], whereas the anion only has a slight effect in determining toxicity [299,300].

The ecotoxicity of quaternary imidazolium, ammonium, quaternary-phosphonium, and pyridinium ILs was determined using two aquatic test models. Results showed that all these ILs had EC50 based toxicities in the range of ~ 104 to 106, which are higher than traditional solvents [301]. Moreover, the *Tox.* decreased as the imidazolium cation alkyl chain length increased for an IL with a chloride anion [280,302]. This tendency has been noted for morpholinium [303], ammonium, pyridinium [304], phosphonium [305], and pyrrolidinium [306] ILs. Additionally, Stolte et al. [307] examined the marine *Tox.* of ILs with various headgroups. The researchers observed a link between IL lipophilicity and (eco)toxicity, wherein the *Tox.* increased as the lipophilicity (hydrophobicity) increased [308]. Including a large alkyl chain also increases the ILs hydrophobicity. The *Tox.* also increased with an expanding alkyl chain length. The alkyl chain number on the cation also improves toxicity.

Additionally, Couling et al. [300] created a quantitative structure–property relationship (QSPR) to evaluate and calculate the *Tox.* of ILs. The QSPR model proposed the subsequent toxicity tendency with cations as: ammonium < pyridinium < imidazolium < triazolium < tetrazolium. However, this trend is uncommon because pyridinium and ammonium ILs are more toxic than imidazolium ILs [307,309]. While the anion performs a secondary part in the toxicity of ILs it can also considerably increase or decrease the toxicity. The toxicity data for marine organisms assembled by Frade et al. [310] reported the anion trend: [Br] < [DCA] < [Cl] < [BF_4] < [PF_6] < [Tf_2N]. Specifically, fluorinated anions, such as Tf_2N and BF_4 are toxic and present a significant environmental hazard [311].

In summary, several test models have been applied to assess toxicity and the test models can react differently to similar ILs. This is why data extrapolation from one particular test model to another must be avoided. However, it is reliably reported that toxicity improves with the length of the alkyl chain and with the alkyl chain number of the cation. Further, the morpholinium cation and the DCA anion seem to be great applicants for decreasing toxic impacts [302,312]. As such, different integrated and efficient methods should be applied to assess toxicity in future research.

11. Conclusions and future prospectives

The effective separation of greenhouse gas including CO_2 from flue gas is a difficult process. The energy amount and the cost for UP_{CO_2} from flue gas is very high, which makes ILs unfavorable for large-scale applications. However, varieties of innovative IL separation methods and materials have been suggested to overcome this issue. This review examined research literature on the CAP_{CO_2} process using ILs. Researchers discussed different tendencies concerning SEL_{CO_2} and S_{CO_2} in numerous ILs, the impact of cations, anions, and functional groups on physical characteristics, *BioDeg*, VOL_{IL}, and *Tox*. of ILs. Additionally, improvements to IL functionalization and supported membrane techniques were discussed in this work.

Based on the solubility tendencies, the S_{CO_2} of traditional ILs-physical methods is minimal at $Post_{com}$ conditions as opposed to the amine

method. Moreover, Henry's constant (H_c) is reduced by increasing the IL_{MFV}, MW_{ILs}, and the accessible volume of ILs. Consequently, the S_{CO_2} in ILs was evaluated on a molarity (mol/m^3) or molality (mol/kg) basis rather than a mole fraction basis. The UP_{CO_2} capacity has been effectively developed by grafting traditional ILs with an amine part, which enables the CO_2 to react chemically with the amine. In comparison to the standard CO_2 amine chemistry, a greater 1:1 reaction stoichiometry may be obtained when the amine is attached to the IL anion.

The SEL_{CO_2} is also an important property for industrial separation methods. The SEL_{CO_2} the assessment indicated that CO_2 is commonly more soluble in ILs compared to other simple gases, such as N_2, H_2, and O_2. On the other hand, the S_{H_2S} and S_{SO_2} gases are also high in ILs. This suggests that the SEL_{CO_2} will be excellent for CO_2/simple-gas systems, while the *SEL* will decrease for CO_2/sour-gas systems. To overcome this challenge, the SEL_{CO_2} may be improved by using low MV_{ILs}. Another obstacle to using grafted and nongrafted ILs in industrial use is their high viscosity. Though, the trends presented in this review can be used to develop ILs with a low viscosity. Additionally, the limited data on *Bio-Deg. Tox.* of ILs indicated that several commonly used ILs are nonbiodegradable and highly toxic. However, some trends highlighted a potential to create essentially secure ILs.

Lastly, there are several barriers that needs to be addressed in future research for the commercialization of IL methods, including:

1) Lack of physicochemical and thermodynamic data. Although a few of the physical characteristics of ILs have been examined, additional information is still needed on viscosity, density, diffusion coefficients, surface tension, specific heat, chemical and thermal stability, water solubility, the heat of fusion, and corrosivity. Rarely were these IL traits articulated, and there were no techniques for calculating precise properties.
2) Lack of data on the stability of ILs. An examination of the long-term thermal and chemical stability of ILs is essential to avoid degradation throughout the absorption and desorption cycles.
3) Lack of scale-up research. To assess ILs' potential on an industrial scale, laboratory-scale methodologies must be scaled up to a pilot plant level. Pilot scale testing is required by the sector before commercialization.
4) A lack of suitable engineering reviews. Organized process engineering research can reduce and manage the expenses associated with manufacturing and ILs-based processes. Unfortunately, the absence of ILs physiochemical properties prevents this kind of research from being conducted at the moment.
5) A lack of safety, environmental, and health studies. To prevent environmental pollution, application ILs' toxicity and biodegradability need to be thoroughly assessed.
6) Durability and breakdown/degradation of ionic liquids: The degradation and disintegration of ILs during the Fenton process, at elevated temperatures, and solid electrolyte interphase have all been covered in several studies. To better guide the design of new ILs, more study is required to better understand the relative impact of the chemical breakdown of the IL ingredients (cation–anion interfacial structure) during the CAP_{CO_2} process at various operating temperatures.

The high cost of ILs. The current lab-scale cost of ILs is approximately $ 1000/kg, which is 100 to 1,000 times more costly than traditional solvents. This rate declines for large-scale IL formation. However, the cost standard for conventional solvents is not estimated because ILs are complicated particles, which require further innovative production and purification stages.

Declaration of Competing Interest

The authors declare that they have no known competing financial interests or personal relationships that could have appeared to influence the work reported in this paper.

Data availability

Data will be made available on request.

Acknowledgments

The authors acknowledge the support provided by Qatar University grant No QUCG-CENG-21/22-3. The statements made herein are solely the responsibility of the authors. Open Access funding provided by the Qatar National Library.

References

[1] Tawalbeh M, et al. The novel contribution of non-noble metal catalysts for intensified carbon dioxide hydrogenation: Recent challenges and opportunities. Energ Conver Manage 2023;279:116755.
[2] Peng B, et al. Can third-party market cooperation solve the dilemma of emissions reduction? A case study of energy investment project conflict analysis in the context of carbon neutrality. Energy 2023;264:126280.
[3] Pang R, et al. The co-occurrent microplastics and nano-CuO showed antagonistic inhibitory effects on bacterial denitrification: Interaction of pollutants and regulations on functional genes. Sci Total Environ 2023;862:160892.
[4] Tongia, R., *Flatten-the-Curve: Why Total Carbon Emissions Matter Much More than "Date of Zero"*. 2021, CSEP Working Paper 14.
[5] Shi W, et al. How to Reduce Carbon Dioxide Emissions from Power Systems in Gansu Province—Analyze from the Life Cycle Perspective. Energies 2022;15(10):3560.
[6] Yang Y, et al. Status and challenges of applications and industry chain technologies of hydrogen in the context of carbon neutrality. J Clean Prod 2022:134347.
[7] Tawalbeh M, et al. The novel advancements of nanomaterials in biofuel cells with a focus on electrodes' applications. Fuel 2022;322:124237.
[8] Han P, et al. A city-level comparison of fossil-fuel and industry processes-induced CO2 emissions over the Beijing-Tianjin-Hebei region from eight emission inventories. Carbon Balance Manag 2020;15(1):1–16.
[9] Soonsawad N, Martinez RM, Schandl H. Material demand, and environmental and climate implications of Australia's building stock: Current status and outlook to 2060. Resour Conserv Recycl 2022;180:106143.
[10] Thiri MA, et al. How social movements contribute to staying within the global carbon budget: Evidence from a qualitative meta-analysis of case studies. Ecol Econ 2022;195:107356.
[11] Gao Y, Gao X, Zhang X. The 2 °C Global Temperature Target and the Evolution of the Long-Term Goal of Addressing Climate Change—From the United Nations Framework Convention on Climate Change to the Paris Agreement. Engineering 2017;3(2):272–8.
[12] Yusuf N, Almomani F. Highly effective hydrogenation of CO2 to methanol over Cu/ZnO/Al2O3 catalyst: A process economy & environmental aspects. Fuel 2023;332:126027.
[13] Alami AH, et al. Materials and logistics for carbon dioxide capture, storage and utilization. Sci Total Environ 2020;717:137221.
[14] Suicmez VS. Feasibility study for carbon capture utilization and storage (CCUS) in the Danish North Sea. J Nat Gas Sci Eng 2019;68:102924.
[15] Chen S, et al. A critical review on deployment planning and risk analysis of carbon capture, utilization, and storage (CCUS) toward carbon neutrality. Renew Sustain Energy Rev 2022;167:112537.
[16] Rozanska X, Wimmer E, de Meyer F. Quantitative kinetic model of CO2 absorption in aqueous tertiary amine solvents. J Chem Inf Model 2021;61(4):1814–24.
[17] Janati S, Aghel B, Shadloo MS. The effect of alkanolamine mixtures on CO2 absorption efficiency in T-Shaped microchannel. Environ Technol Innov 2021;24:102006.
[18] Perumal M, Jayaraman D. Understanding the physical and thermodynamic properties of monoethanolamine-ionic liquids for solvent screening in CO2 capture process. Asia Pac J Chem Eng 2022;17(3):e2775.
[19] Ye J, et al. Novel biphasic solvent with tunable phase separation for CO2 capture: Role of water content in mechanism, kinetics, and energy penalty. Environ Sci Tech 2019;53(8):4470–9.
[20] Liu S, et al. Kinetics and new Brønsted correlations study of CO2 absorption into primary and secondary alkanolamine with and without steric-hindrance. Sep Purif Technol 2020;233:115998.
[21] Silva-Beard A, Flores-Tlacuahuac A, Rivera-Toledo M. Optimal computer-aided molecular design of ionic liquid mixtures for post-combustion carbon dioxide capture. Comput Chem Eng 2022;157:107622.
[22] Panja P, McPherson B, Deo M. Techno-economic analysis of amine-based CO2 capture technology: hunter plant case study. Carbon Capture Sci Technol 2022;3:100041.
[23] Rochelle GT. Amine scrubbing for CO2 capture. Science 2009;325(5948):1652–4.
[24] Rahimi M, et al. Electrochemical carbon capture processes for mitigation of CO 2 emissions. Chem Soc Rev 2022.

[25] Mulu E, M'Arimi MM, Ramkat RC. A review of recent developments in application of low cost natural materials in purification and upgrade of biogas. Renew Sustain Energy Rev 2021;145:111081.
[26] Zhao P, et al. The latest development on amine functionalized solid adsorbents for post-combustion CO2 capture: Analysis review. Chin J Chem Eng 2021;35:17–43.
[27] Rasouli H, Nguyen K, Iliuta MC. Recent advancements in carbonic anhydrase immobilization and its implementation in CO2 capture technologies: A review. Sep Purif Technol 2022:121299.
[28] Tawalbeh M, et al. Modeling the transport of CO2, N2, and their binary mixtures through highly permeable silicalite-1 membranes using Maxwell−Stefan equations. Chemosphere 2021;263:127935.
[29] Liu J, et al. Applications of metal–organic framework composites in CO2 capture and conversion. Chin Chem Lett 2021;32(2):649–59.
[30] Bernard FL, et al. Polyurethane-based poly (ionic liquid) s for CO2 removal from natural gas. Appl Poly 2019;136(20):47536.
[31] Tawalbeh M, et al. Lignin/zirconium phosphate/ionic liquids-based proton conducting membranes for high-temperature PEM fuel cells applications. Energy 2022;260:125237.
[32] Ka'ki A, et al. Proton conduction of novel calcium phosphate nanocomposite membranes for high temperature PEM fuel cells applications. Int J Hydrogen Energy 2021;46(59):30641–57.
[33] Dubey A, Arora A. Advancements in carbon capture technologies: A review. J Clean Prod 2022:133932.
[34] Berthod A, Ruiz-Angel MJ, Carda-Broch S. Recent advances on ionic liquid uses in separation techniques. J Chromatogr A 2018;1559:2–16.
[35] Freemantle M. Designer solvents-Ionic liquids may boost clean technology development. Chem Eng News 1998;76(13):32–7.
[36] Singh SK, Savoy AW. Ionic liquids synthesis and applications: An overview. J Mol Liq 2020;297:112038.
[37] Chen Y, Mu T. Revisiting greenness of ionic liquids and deep eutectic solvents. Green Chemical Engineering 2021;2(2):174–86.
[38] Zafar A, et al. Synthesis, structural analysis, electrochemical and magnetic properties of tetrachloroferrate (III) ionic liquids. New J Chem 2021.
[39] Nikfarjam N, et al. Antimicrobial ionic liquid-based materials for biomedical applications. Adv Funct Mater 2021;31(42):2104148.
[40] Sajid M. Magnetic ionic liquids in analytical sample preparation: A literature review. TrAC Trends Anal Chem 2019;113:210–23.
[41] Dhameliya TM, et al. Recent advancements in applications of ionic liquids in synthetic construction of heterocyclic scaffolds: A spotlight. J Mol Liq 2022;348:118329.
[42] Ashouri R, et al. Dynamic and static removal of benzene from air based on task-specific ionic liquid coated on MWCNTs by sorbent tube-headspace solid-phase extraction procedure. Int J Environ Sci Technol 2021;18(8):2377–90.
[43] Rykowska I, Nowak I, Wasiak W. Recent trends in the application of ionic liquids for micro extraction techniques. Recent Adv Anal Tech 2019;3:61–133.
[44] Gomes JM, Silva SS, Reis RL. Biocompatible ionic liquids: fundamental behaviours and applications. Chem Soc Rev 2019;48(15):4317–35.
[45] Claus J, Sommer FO, Kragl U. Ionic liquids in biotechnology and beyond. Solid State Ion 2018;314:119–28.
[46] Elmobarak WF, Almomani F. Evaluation of the efficiency of ionic liquids in the demulsification of oil-in-water emulsions. Environ Technol Innov 2021;24:102003.
[47] Bahadur I, Phadagi R. Ionic Liquids as Environmental Benign Solvents for Cellulose Chemistry: A Review. Solvents: Ionic Liquids and Solvent Effects; 2019. p. 1–12.
[48] Yim J-H, Oh B-K, Lim JS. Solubility Measurement and Correlation of CO2 in bis (pentafluoroethylsulfonyl) imide ([BETI]) Anion-Based Ionic Liquids:[EMIM][BETI],[BMIM][BETI],[HMIM][BETI]. J Chem Eng Data 2020;65(9):4378–86.
[49] Alkhatib II, et al. Screening of ionic liquids and deep eutectic solvents for physical CO2 absorption by Soft-SAFT using key performance indicators. J Chem Eng Data 2020;65(12):5844–61.
[50] Carvalho PJ, et al. High pressure phase behavior of carbon dioxide in 1-butyl-3-methylimidazolium bis (trifluoromethylsulfonyl) imide and 1-butyl-3-methylimidazolium dicyanamide ionic liquids. J Supercrit Fluids 2009;50(2):105–11.
[51] Wu G, et al. The CO(2) Absorption in Flue Gas Using Mixed Ionic Liquids. Molecules 2020;25(5).
[52] Wang Y, et al. Two-dimensional ionic liquids with an anomalous stepwise melting process and ultrahigh CO2 adsorption capacity. Cell Reports Phys Sci 2022;3(7):100979.
[53] Wang J, et al. Recent development of ionic liquid membranes. Green Energy Environ 2016;1(1):43–61.
[54] Phan L, et al. Switchable solvents consisting of amidine/alcohol or guanidine/alcohol mixtures. Ind Eng Chem Res 2008;47(3):539–45.
[55] Brzęczek-Szafran A, et al. Combining amino acids and carbohydrates into readily biodegradable, task specific ionic liquids. RSC Adv 2020;10(31):18355–9.
[56] Aghaie M, Rezaei N, Zendehboudi S. A systematic review on CO2 capture with ionic liquids: Current status and future prospects. Renew Sustain Energy Rev 2018;96:502–25.
[57] Wu Y, et al. Recent advances in carbon dioxide capture and utilization with amines and ionic liquids. Green Chem Eng 2020;1(1):16–32.
[58] Eren BM, Taspinar N, Gokmenoglu KK. The impact of financial development and economic growth on renewable energy consumption: Empirical analysis of India. Sci Total Environ 2019;663:189–97.
[59] Jackson R, et al. Global fossil carbon emissions rebound near pre-COVID-19 levels. Environ Res Lett 2022;17(3):031001.
[60] Zhou L, Fan J, Shang X. CO2 capture and separation properties in the ionic liquid 1-n-butyl-3-methylimidazolium nonafluorobutylsulfonate. Materials 2014;7(5):3867–80.
[61] Palanisamy D, Ayalur BK. Impact of condensate cooled air purging on indoor air quality in an air conditioned laboratory. Build Environ 2021;188:107511.
[62] Ritchie H, Roser M, Rosado P. CO_2 and greenhouse gas emissions. Our World in Data 2020.
[63] Doo SS, Edmunds PJ, Carpenter RC. Ocean acidification effects on in situ coral reef metabolism. Sci Rep 2019;9(1):12067.
[64] Tan Z, et al. Attapulgite as a cost-effective catalyst for low-energy consumption amine-based CO2 capture. Sep Purif Technol 2022;298:121577.
[65] Vaidya PD, Kenig EY. CO2-alkanolamine reaction kinetics: a review of recent studies. Chem Eng Technol: Ind Chem-Plant Equipment-Process Eng-Biotechnol 2007;30(11):1467–74.
[66] Gautam A, Mondal MK. Review of recent trends and various techniques for CO2 capture: Special emphasis on biphasic amine solvents. Fuel 2023;334:126616.
[67] Fernández-González J, et al. Hydrogen utilization in the sustainable manufacture of CO2-based methanol. Ind Eng Chem Res 2022;61(18):6163–72.
[68] Ellaf A, et al. Energy, exergy, economic, environment, exergo-environment based assessment of amine-based hybrid solvents for natural gas sweetening. Chemosphere 2023;313:137426.
[69] Fan H, et al. Performance comparation of MEA and EDA in electrochemically-mediated amine regeneration for CO2 capture. Sep Purif Technol 2023:123282.
[70] Liu C, et al. Experimental study and modified modeling on effect of SO2 on CO2 absorption using amine solution. Chem Eng J 2022;448:137751.
[71] Davidson, R.M., *Post-combustion carbon capture from coal fired plants-solvent scrubbing*. 2007.
[72] Liu J, et al. The chemical CO2 capture by carbonation-decarbonation cycles. J Environ Manage 2020;260:110054.
[73] Madejski P, et al. Methods and techniques for CO2 capture: Review of potential solutions and applications in modern energy technologies. Energies 2022;15(3):887.
[74] Wu X, et al. Solvent-based post-combustion CO2 capture for power plants: A critical review and perspective on dynamic modelling, system identification, process control and flexible operation. Appl Energy 2020;257:113941.
[75] Raganati F, Miccio F, Ammendola P. Adsorption of carbon dioxide for post-combustion capture: A review. Energy Fuel 2021;35(16):12845–68.
[76] Rosner F, et al. Thermo-economic analyses of isothermal water gas shift reactor integrations into IGCC power plant. Appl Energy 2020;277:115500.
[77] Abdelaal M, et al. Characteristics and flame appearance of oxy-fuel combustion using flue gas recirculation. Fuel 2021;297:120775.
[78] Zakrzewska ME, et al. High-Pressure Phase Equilibrium Studies of Multicomponent (Alcohol-Water-Ionic Liquid-CO2) Systems. C 2020;6(1):9.
[79] Kroon MC, et al. High-pressure phase behavior of systems with ionic liquids: Part V. The binary system carbon dioxide+ 1-butyl-3-methylimidazolium tetrafluoroborate. J Chem Eng Data 2005;50(1):173–6.
[80] Chen T, et al. Effects of the structure on physicochemical properties and CO2 absorption of hydroxypyridine anion-based protic ionic liquids. J Mol Liq 2022;362:119743.
[81] Hayes R, Warr GG, Atkin R. Structure and nanostructure in ionic liquids. Chem Rev 2015;115(13):6357–426.
[82] Aki SN, et al. High-pressure phase behavior of carbon dioxide with imidazolium-based ionic liquids. J Phys Chem B 2004;108(52):20355–65.
[83] Li B, et al. High CO2 absorption capacity of metal-based ionic liquids: A molecular dynamics study. Green Energy Environ 2021;6(2):253–60.
[84] Shaikh AR, et al. Selective absorption of H2S and CO2 by azole based protic ionic liquids: A combined density functional theory and molecular dynamics study. J Mol Liq 2022;367:120558.
[85] Kazarian, S.G., B.J. Briscoe, and T. Welton, Combining ionic liquids and supercritical fluids: in situ ATR-IR study of CO2 dissolved in two ionic liquids at high pressuresElectronic supplementary information (ESI) available: schematic view of the miniature high-pressure flow cell. See *http://www*. rsc. org/suppdata/cc/b0/b005514j. Chemical Communications, 2000(20): p. 2047-2048.
[86] Chen T, Wu X, Xu Y. Effects of the structure on physicochemical properties and CO2 absorption of hydroxypyridine anion-based protic ionic liquids. J Mol Liq 2022;362:119743.
[87] Shaikh AR, et al. Amino acid ionic liquids as potential candidates for CO2 capture: combined density functional theory and molecular dynamics simulations. Chem Phys Lett 2020;745:137239.
[88] Kanakubo M, et al. Solution structures of 1-butyl-3-methylimidazolium hexafluorophosphate ionic liquid saturated with CO2: experimental evidence of specific anion− CO2 interaction. J Phys Chem B 2005;109(29):13847–50.
[89] Zunita M, et al. *Integrated metal organic framework/ionic liquid-based composite membrane for CO2 separation.* Chemical Engineering Journal. Advances 2022:100320.
[90] Zailani NHZO, et al. Experimental investigation on thermophysical properties of ammonium-based protic ionic liquids and their potential ability towards CO2 capture. Molecules 2022;27(3):851.
[91] Farsi M, Soroush E. CO2 absorption by ionic liquids and deep eutectic solvents. In: Advances in Carbon Capture. Elsevier; 2020. p. 89–105.
[92] Wang L-Y, et al. CO2/CH4 and H2S/CO2 Selectivity by Ionic Liquids in Natural Gas Sweetening. Energy Fuel 2018;32(1):10–23.
[93] Maiti, A., *Cover Picture: Theoretical Screening of Ionic Liquid Solvents for Carbon Capture (ChemSusChem 7/2009)*. ChemSusChem: Chemistry & Sustainability Energy & Materials, 2009. 2(7): p. 597-597.

[94] Sistla YS, Khanna A. Validation and prediction of the temperature-dependent Henry's constant for CO2–ionic liquid systems using the conductor-like screening model for realistic solvation (COSMO-RS). J Chem Eng Data 2011;56(11):4045–60.
[95] Zhang X, Liu Z, Wang W. Screening of ionic liquids to capture CO2 by COSMO-RS and experiments. AIChE J 2008;54(10):2717–28.
[96] Sosa JE, et al. Design of ionic liquids for fluorinated gas absorption: COSMO-RS selection and solubility experiments. Environ Sci Tech 2022;56(9):5898–909.
[97] Palomar J, et al. Understanding the physical absorption of CO2 in ionic liquids using the COSMO-RS method. Ind Eng Chem Res 2011;50(6):3452–63.
[98] Hospital-Benito D, et al. Improvement of CO2 capture processes by tailoring the reaction enthalpy of Aprotic N-Heterocyclic anion-based ionic liquids. Chem Eng J Adv 2022;10:100291.
[99] Jacquemin J, et al. Density and viscosity of several pure and water-saturated ionic liquids. Green Chem 2006;8(2):172–80.
[100] Almantariotis D, et al. Effect of fluorination and size of the alkyl side-chain on the solubility of carbon dioxide in 1-alkyl-3-methylimidazolium bis (trifluoromethylsulfonyl) amide ionic liquids. J Phys Chem B 2010;114(10):3608–17.
[101] Ramdin M, de Loos TW, Vlugt TJH. State-of-the-Art of CO2 Capture with Ionic Liquids. Ind Eng Chem Res 2012;51(24):8149–77.
[102] Shimoyama Y, Ito A. Predictions of cation and anion effects on solubilities, selectivities and permeabilities for CO2 in ionic liquid using COSMO based activity coefficient model. Fluid Phase Equilib 2010;297(2):178–82.
[103] Zhang J, et al. The interaction nature between hollow silica-based porous ionic liquids and CO2: A DFT study. J Mol Graph Model 2020;100:107694.
[104] Cadena C, et al. Why is CO2 so soluble in imidazolium-based ionic liquids? J Am Chem Soc 2004;126(16):5300–8.
[105] Shamair Z, et al. Theoretical and experimental investigation of CO2 separation from CH4 and N2 through supported ionic liquid membranes. Appl Energy 2020;268:115016.
[106] Jiang Y, et al. Hydrogen bond donor functionalized poly(ionic liquids)@MIL-101 for the CO2 capture and improving the catalytic CO2 conversion with epoxide. J Colloid Interface Sci 2022;618:22–33.
[107] Zhai Z, et al. Combined Surface Light Scattering and Pendant-Drop Experiments for the Determination of Viscosity and Surface Tension of High-Viscosity Fluids Demonstrated for Ionic Liquids. Int J Thermophys 2022;43(12):178.
[108] Abourehab MA, et al. Efficiency development of surface tension for different ionic liquids through novel model of Machine learning Technique: Application of in-thermal engineering. J Mol Liq 2022;367:120391.
[109] Shojaeian A, Asadizadeh M. Prediction of surface tension of the binary mixtures containing ionic liquid using heuristic approaches; an input parameters investigation. J Mol Liq 2020;298:111976.
[110] Dębski B, et al. Thermodynamic interpretation and prediction of CO2 solubility in imidazolium ionic liquids based on regular solution theory. J Mol Liq 2019;291:110477.
[111] Nikolenko MV, et al. Synthesis of calcium orthophosphates by chemical precipitation in aqueous solutions: The effect of the acidity, Ca/P molar ratio, and temperature on the phase composition and solubility of precipitates. Processes 2020;8(9):1009.
[112] Lin W, et al. Tuning the Capture of CO2 through Entropic Effect Induced by Reversible Trans-Cis Isomerization of Light-Responsive Ionic Liquids. J Phys Chem Lett 2019;10(12):3346–51.
[113] Blanchard LA, Gu Z, Brennecke JF. High-pressure phase behavior of ionic liquid/CO2 systems. J Phys Chem B 2001;105(12):2437–44.
[114] Kumełan J, et al. Solubility of the single gases carbon dioxide and hydrogen in the ionic liquid [bmpy][Tf2N]. J Chem Eng Data 2010;55(1):165–72.
[115] Carvalho PJ, Coutinho JA. On the nonideality of CO2 solutions in ionic liquids and other low volatile solvents. J Phys Chem Lett 2010;1(4):774–80.
[116] Brennecke JF, Gurkan BE. Ionic liquids for CO2 capture and emission reduction. J Phys Chem Lett 2010;1(24):3459–64.
[117] Suzuki Y, et al. CO2/Hydrocarbon Selectivity of Trihexyl (tetradecyl) phosphonium-Based Ionic Liquids. Ind Eng Chem Res 2022;61(44):16584–92.
[118] Aghaie M, Zendehboudi S. Estimation of CO2 solubility in ionic liquids using connectionist tools based on thermodynamic and structural characteristics. Fuel 2020;279:117984.
[119] Domańska U, Królikowska M. Density and viscosity of binary mixtures of {1-butyl-3-methylimidazolium thiocyanate+ 1-heptanol, 1-octanol, 1-nonanol, or 1-decanol}. J Chem Eng Data 2010;55(9):2994–3004.
[120] Gonçalves F, et al. Pressure–volume–temperature measurements of phosphonium-based ionic liquids and analysis with simple equations of state. J Chem Thermodyn 2011;43(6):914–29.
[121] Song T, Lubben MJ, Brennecke JF. Solubility of argon, krypton and xenon in ionic liquids. Fluid Phase Equilib 2020;504:112334.
[122] Zhao YH, Abraham MH, Zissimos AM. Fast calculation of van der Waals volume as a sum of atomic and bond contributions and its application to drug compounds. J Org Chem 2003;68(19):7368–73.
[123] Bondi AV. van der Waals volumes and radii. J Phys Chem 1964;68(3):441–51.
[124] Shannon MS, et al. Free volume as the basis of gas solubility and selectivity in imidazolium-based ionic liquids. Ind Eng Chem Res 2012;51(15):5565–76.
[125] Karadas F, Atilhan M, Aparicio S. Review on the use of ionic liquids (ILs) as alternative fluids for CO2 capture and natural gas sweetening. Energy Fuel 2010;24(11):5817–28.
[126] Shiflett MB, Yokozeki A. Solubilities and diffusivities of carbon dioxide in ionic liquids:[bmim][PF6] and [bmim][BF4]. Ind Eng Chem Res 2005;44(12):4453–64.
[127] Perez-Salado Kamps A, et al. Solubility of CO2 in the ionic liquid [bmim][PF6]. J Chem Eng Data 2003;48(3):746–9.
[128] Anderson JL, Dixon JK, Brennecke JF. Solubility of CO2, CH4, C2H6, C2H4, O2, and N2 in 1-Hexyl-3-methylpyridinium Bis (trifluoromethylsulfonyl) imide: Comparison to Other Ionic Liquids. Acc Chem Res 2007;40(11):1208–16.
[129] Kilaru PK, Scovazzo P. Correlations of low-pressure carbon dioxide and hydrocarbon solubilities in imidazolium-, phosphonium-, and ammonium-based room-temperature ionic liquids. Part 2. Using activation energy of viscosity. Ind Eng Chem Res 2008;47(3):910–9.
[130] Carvalho PJ, et al. High carbon dioxide solubilities in trihexyltetradecylphosphonium-based ionic liquids. J Supercrit Fluids 2010;52(3):258–65.
[131] Yazdizadeh M, Rahmani F, Forghani AA. Thermodynamic modeling of CO2 solubility in ionic liquid ([Cn-mim] [Tf2N]; n=2, 4, 6, 8) with using Wong-Sandler mixing rule, Peng-Rabinson equation of state (EOS) and differential evolution (DE) method. Korean J Chem Eng 2011;28(1):246–51.
[132] Wang J, et al. Modeling of pvT behavior of semi-crystalline polymer based on the two-domain Tait equation of state for injection molding. Mater Des 2019;183:108149.
[133] Zhang S, et al. Physical Properties of Ionic Liquids: Database and Evaluation. J Phys Chem Ref Data 2006;35:1475.
[134] Anthony JL, et al. Anion effects on gas solubility in ionic liquids. J Phys Chem B 2005;109(13):6366–74.
[135] Lei Z, Dai C, Chen B. Gas Solubility in Ionic Liquids. Chem Rev 2014;114(2):1289–326.
[136] Kumełan J, et al. Solubility of CO in the ionic liquid [bmim][PF6]. Fluid Phase Equilib 2005;228:207–11.
[137] Carvalho PJ, Coutinho JA. The polarity effect upon the methane solubility in ionic liquids: a contribution for the design of ionic liquids for enhanced CO 2/CH 4 and H 2 S/CH 4 selectivities. Energ Environ Sci 2011;4(11):4614–9.
[138] Kumełan J, et al. Solubility of H2 in the ionic liquid [hmim][Tf2N]. J Chem Eng Data 2006;51(4):1364–7.
[139] Biswas R. Molecular dynamics simulations and COSMO-RS method for CO2 capture in imidazolium and pyrrolidinium-based room-temperature ionic liquids. J Mol Model 2022;28(8):1–8.
[140] Kumełan J, et al. Solubility of the single gases H2 and CO in the ionic liquid [bmim][CH3SO4]. Fluid Phase Equilib 2007;260(1):3–8.
[141] Jacquemin J, et al. Solubility of carbon dioxide, ethane, methane, oxygen, nitrogen, hydrogen, argon, and carbon monoxide in 1-butyl-3-methylimidazolium tetrafluoroborate between temperatures 283 K and 343 K and at pressures close to atmospheric. J Chem Thermodyn 2006;38(4):490–502.
[142] Jacquemin J, et al. Low-pressure solubilities and thermodynamics of solvation of eight gases in 1-butyl-3-methylimidazolium hexafluorophosphate. Fluid Phase Equilib 2006;240(1):87–95.
[143] Jacquemin J, et al. Influence of the cation on the solubility of CO 2 and H 2 in ionic liquids based on the bis (trifluoromethylsulfonyl) imide anion. J Solution Chem 2007;36(8):967–79.
[144] Yokozeki A, Shiflett MB. Hydrogen purification using room-temperature ionic liquids. Appl Energy 2007;84(3):351–61.
[145] Ying W, et al. Ionic liquid selectively facilitates CO2 transport through graphene oxide membrane. ACS Nano 2018;12(6):5385–93.
[146] Shiflett MB, Yokozeki A. Separation of CO2 and H2S using room-temperature ionic liquid [bmim][PF6]. Fluid Phase Equilib 2010;294(1–2):105–13.
[147] Barzegar B, Feyzi F. Effect of ionic liquids in carbon nanotube bundles on CO2, H2S, and N2 separation from CH4: A computational study. J Chem Phys 2021;154(19):194504.
[148] Kumełan J, et al. Solubility of oxygen in the ionic liquid [bmim][PF6]: Experimental and molecular simulation results. J Chem Thermodyn 2005;37(6):595–602.
[149] Costa Gomes M. Low-pressure solubility and thermodynamics of solvation of carbon dioxide, ethane, and hydrogen in 1-hexyl-3-methylimidazolium bis (trifluoromethylsulfonyl) amide between temperatures of 283 K and 343 K. J Chem Eng Data 2007;52(2):472–5.
[150] Anthony JL, Maginn EJ, Brennecke JF. Solubilities and thermodynamic properties of gases in the ionic liquid 1-n-butyl-3-methylimidazolium hexafluorophosphate. J Phys Chem B 2002;106(29):7315–20.
[151] Abbas M, et al. Highly stable-silica encapsulating magnetite nanoparticles (Fe3O4/SiO2) synthesized using single surfactantless-polyol process. Ceram Int 2014;40(1):1379–85.
[152] Guo Z, et al. Ionic liquid tuning nanocage size of MOFs through a two-step adsorption/infiltration strategy for enhanced gas screening of mixed-matrix membranes. J Membr Sci 2020;605:118101.
[153] Camper D, et al. Gas solubilities in room-temperature ionic liquids. Ind Eng Chem Res 2004;43(12):3049–54.
[154] Finotello A, et al. Room-temperature ionic liquids: temperature dependence of gas solubility selectivity. Ind Eng Chem Res 2008;47(10):3453–9.
[155] Bara JE, et al. Enhanced CO2 separation selectivity in oligo (ethylene glycol) functionalized room-temperature ionic liquids. Ind Eng Chem Res 2007;46(16):5380–6.
[156] Carlisle TK, et al. Interpretation of CO2 solubility and selectivity in nitrile-functionalized room-temperature ionic liquids using a group contribution approach. Ind Eng Chem Res 2008;47(18):7005–12.
[157] Mahurin SM, et al. Benzyl-functionalized room temperature ionic liquids for CO2/N2 separation. Ind Eng Chem Res 2011;50(24):14061–9.

[158] Hert DG, et al. Enhancement of oxygen and methane solubility in 1-hexyl-3-methylimidazolium bis (trifluoromethylsulfonyl) imide using carbon dioxide. Chem Commun 2005;20:2603–5.
[159] Shi W, Maginn EJ. Molecular simulation and regular solution theory modeling of pure and mixed gas absorption in the ionic liquid 1-n-hexyl-3-methylimidazolium bis (trifluoromethylsulfonyl) amide ([hmim][Tf2N]). J Phys Chem B 2008;112 (51):16710–20.
[160] Maginn EJ. Molecular simulation of ionic liquids: current status and future opportunities. J Phys Condens Matter 2009;21(37):373101.
[161] Shiflett MB, Niehaus AMS, Yokozeki A. Separation of CO2 and H2S using room-temperature ionic liquid [bmim][MeSO4]. J Chem Eng Data 2010;55(11): 4785–93.
[162] Jalili AH, et al. Solubility of CO2 in 1-(2-hydroxyethyl)-3-methylimidazolium ionic liquids with different anions. J Chem Thermodyn 2010;42(6):787–91.
[163] Kumełan J, Tuma D, Maurer G. Simultaneous solubility of carbon dioxide and hydrogen in the ionic liquid [hmim][Tf2N]: Experimental results and correlation. Fluid Phase Equilib 2011;311:9–16.
[164] Kim Y, et al. Solubility of mixed gases containing carbon dioxide in ionic liquids: Measurements and predictions. Fluid Phase Equilib 2007;256(1–2):70–4.
[165] Weingärtner H. Understanding ionic liquids at the molecular level: facts, problems, and controversies. Angew Chem Int Ed 2008;47(4):654–70.
[166] Moganty SS, Baltus RE. Diffusivity of carbon dioxide in room-temperature ionic liquids. Ind Eng Chem Res 2010;49(19):9370–6.
[167] Crosthwaite JM, et al. Phase transition and decomposition temperatures, heat capacities and viscosities of pyridinium ionic liquids. J Chem Thermodyn 2005;37 (6):559–68.
[168] Tsunashima K, Sugiya M. Physical and electrochemical properties of low-viscosity phosphonium ionic liquids as potential electrolytes. Electrochem Commun 2007;9 (9):2353–8.
[169] Yoshida Y, et al. Superionic conduction over a wide temperature range in a metal–organic framework impregnated with ionic liquids. Angew Chem Int Ed 2019;58(32):10909–13.
[170] Zhao Z, et al. Molecular Simulation and Experimental Study on Low-Viscosity Ionic Liquids for High-Efficient Capturing of CO2. Energy Fuel 2022;36(3): 1604–13.
[171] Harris KR, Kanakubo M, Woolf LA. Temperature and pressure dependence of the viscosity of the ionic liquids 1-methyl-3-octylimidazolium hexafluorophosphate and 1-methyl-3-octylimidazolium tetrafluoroborate. J Chem Eng Data 2006;51 (3):1161–7.
[172] Harris KR, Kanakubo M, Woolf LA. Temperature and pressure dependence of the viscosity of the ionic liquid 1-butyl-3-methylimidazolium tetrafluoroborate: viscosity and density relationships in ionic liquids. J Chem Eng Data 2007;52(6): 2425–30.
[173] Gardas RL, Coutinho JA. A group contribution method for viscosity estimation of ionic liquids. Fluid Phase Equilib 2008;266(1–2):195–201.
[174] Gardas RL, Coutinho JA. Group contribution methods for the prediction of thermophysical and transport properties of ionic liquids. AIChE J 2009;55(5): 1274–90.
[175] Zailani, N.H., et al. Experimental Investigation on Thermophysical Properties of Ammonium-Based Protic Ionic Liquids and Their Potential Ability towards CO2 Capture. Molecules, 2022. 27, DOI: 10.3390/molecules27030851.
[176] Hou Y, Baltus RE. Experimental measurement of the solubility and diffusivity of CO2 in room-temperature ionic liquids using a transient thin-liquid-film method. Ind Eng Chem Res 2007;46(24):8166–75.
[177] Ferguson L, Scovazzo P. Solubility, diffusivity, and permeability of gases in phosphonium-based room temperature ionic liquids: data and correlations. Ind Eng Chem Res 2007;46(4):1369–74.
[178] Morgan D, Ferguson L, Scovazzo P. Diffusivities of gases in room-temperature ionic liquids: data and correlations obtained using a lag-time technique. Ind Eng Chem Res 2005;44(13):4815–23.
[179] Earle MJ, et al. The distillation and volatility of ionic liquids. Nature 2006;439 (7078):831–4.
[180] MSS Esperança, J., et al., *Volatility of Aprotic Ionic Liquids A Review*. Journal of Chemical & Engineering Data, 2010. 55(1): p. 3-12.
[181] Armstrong JP, et al. Vapourisation of ionic liquids. PCCP 2007;9(8):982–90.
[182] Rai N, Maginn EJ. Vapor–liquid coexistence and critical behavior of ionic liquids via molecular simulations. J Phys Chem Lett 2011;2(12):1439–43.
[183] Köddermann T, Paschek D, Ludwig R. Ionic liquids: Dissecting the enthalpies of vaporization. ChemPhysChem 2008;9(4):549–55.
[184] Ludwig R, Kragl U. Do we understand the volatility of ionic liquids? Angew Chem Int Ed 2007;46(35):6582–4.
[185] Rebelo LP, et al. On the critical temperature, normal boiling point, and vapor pressure of ionic liquids. J Phys Chem B 2005;109(13):6040–3.
[186] Khan Swati I, et al. Non-dispersive solvent absorption of post-combustion CO2 in membrane contactors using ionic liquids. J Mol Liq 2022;351:118566.
[187] Fumino K, et al. Estimating Enthalpies of Vaporization of Imidazolium-Based Ionic Liquids from Far-Infrared Measurements. ChemPhysChem 2010;11(8): 1623–6.
[188] Deyko A, et al. Measuring and predicting Δ vap H 298 values of ionic liquids. PCCP 2009;11(38):8544–55.
[189] Rocha MA, et al. High-accuracy vapor pressure data of the extended [C n C1im] [Ntf2] ionic liquid series: trend changes and structural shifts. J Phys Chem B 2011;115(37):10919–26.
[190] Kianfar E, Mafi S. Ionic liquids: properties, application, and synthesis. Fine Chemical Engineering 2021:22–31.
[191] Noorani N, Mehrdad A, Zarei Diznab R. Thermodynamic study on carbon dioxide absorption in vinyl imidazolium–amino acid ionic liquids. Fluid Phase Equilib 2022;557:113433.
[192] Bates ED, et al. CO2 capture by a task-specific ionic liquid. J Am Chem Soc 2002; 124(6):926–7.
[193] Davis H, James J. Task-specific ionic liquids. Chem Lett 2004;33(9):1072–7.
[194] Ding M, Jiang H-L. Incorporation of imidazolium-based poly (ionic liquid) s into a metal–organic framework for CO2 capture and conversion. ACS Catal 2018;8(4): 3194–201.
[195] Chen C, et al. Guanidine-embedded poly(ionic liquid) as a versatile precursor for self-templated synthesis of nitrogen-doped carbons: Tailoring the microstructure for enhanced CO2 capture. Fuel 2022;329:125357.
[196] Shohrat A, et al. Mechanism study on CO2 capture by ionic liquids made from TFA blended with MEA and MDEA. Int J Greenhouse Gas Control 2022;119: 103709.
[197] Camper D, et al. Room-temperature ionic liquid− amine solutions: tunable solvents for efficient and reversible capture of CO2. Ind Eng Chem Res 2008;47 (21):8496–8.
[198] Sánchez LG, Meindersma G, De Haan A. Solvent properties of functionalized ionic liquids for CO2 absorption. Chem Eng Res Des 2007;85(1):31–9.
[199] Fatima SS, et al. Development and progress of functionalized silica-based adsorbents for CO2 capture. J Mol Liq 2021;338:116913.
[200] Yu G, et al. Structure, interaction and property of amino-functionalized imidazolium ILs by molecular dynamics simulation and Ab initio calculation. AIChE J 2007;53(12):3210–21.
[201] Gutowski KE, Maginn EJ. Amine-functionalized task-specific ionic liquids: a mechanistic explanation for the dramatic increase in viscosity upon complexation with CO2 from molecular simulation. J Am Chem Soc 2008;130(44):14690–704.
[202] Gurkan BE, et al. Equimolar CO2 absorption by anion-functionalized ionic liquids. J Am Chem Soc 2010;132(7):2116–7.
[203] Goodrich BF, et al. Experimental measurements of amine-functionalized anion-tethered ionic liquids with carbon dioxide. Ind Eng Chem Res 2011;50(1):111–8.
[204] Shi G, et al. Efficient capture of CO2 from flue gas at high temperature by tunable polyamine-based hybrid ionic liquids. AIChE J 2020;66(1):e16779.
[205] Voskian S, et al. Amine-based ionic liquid for CO2 capture and electrochemical or thermal regeneration. ACS Sust Chem Eng 2020;8(22):8356–61.
[206] Shahrom MSR, et al. Amino acid based poly (ionic liquid) materials for CO2 capture: effect of anion. J Mol Liquids 2019;276:644–52.
[207] Hafizi A, et al. Synthesis, property analysis and absorption efficiency of newly prepared tricationic ionic liquids for CO2 capture. J Mol Liquids 2021;324: 115108.
[208] Amiri N, et al. Design of absorption process for CO2 capture using cyano based anion ionic liquid. Chem Eng Res Design 2021;169:239–49.
[209] Wasewar K. Carbon Dioxide Capture by Ionic Liquids. In: Advances in Carbon Capture and Utilization. Springer; 2021. p. 147–94.
[210] Maginn, E.J., *Design and evaluation of ionic liquids as novel CO2 absorbents*. 2004, University of Notre Dame (US).
[211] Shiflett MB, et al. Phase behavior of carbon dioxide+[bmim][Ac] mixtures. J Chem Thermodyn 2008;40(1):25–31.
[212] Páez, E.I., et al., *Enhanced CO2 capture kinetics by using macroporous carbonized natural fibers impregnated with an ionic liquid*. 2022: p. 118602.
[213] Wang C, et al. Carbon dioxide capture by superbase-derived protic ionic liquids. Angew Chem 2010;122(34):6114–7.
[214] Zhang W, et al. CO2 capture with polyamine-based protic ionic liquid functionalized mesoporous silica. J CO2 Utilization 2019;34:606–15.
[215] Torralba-Calleja E, Skinner J, Gutiérrez-Tauste D. CO2 capture in ionic liquids: a review of solubilities and experimental methods. J Chem 2013;2013.
[216] Heldebrant DJ, et al. The reaction of 1, 8-diazabicyclo [5.4. 0] undec-7-ene (DBU) with carbon dioxide. J Org Chem 2005;70(13):5335–8.
[217] Latini G, et al. Efficient and reversible CO2 capture in bio-based ionic liquids solutions. J CO2 Util 2022;55:101815.
[218] Elliott, T., *An investigation into switchable polarity ionic liquids using mixed carbamates*. 2019.
[219] Heldebrant DJ, et al. Organic liquid CO 2 capture agents with high gravimetric CO 2 capacity. Energ Environ Sci 2008;1(4):487–93.
[220] Blasucci VM, et al. Reversible ionic liquids designed for facile separations. Fluid Phase Equilib 2010;294(1–2):1–6.
[221] Jessop PG, Mercer SM, Heldebrant DJ. CO 2-triggered switchable solvents, surfactants, and other materials. Energ Environ Sci 2012;5(6):7240–53.
[222] Latini G, et al. Efficient and reversible CO2 capture in bio-based ionic liquids solutions. J CO2 Utilization 2022;55:101815.
[223] Chao C, et al. Post-combustion carbon capture. Renew Sustain Energy Rev 2021; 138:110490.
[224] Haider J, et al. State-of-the-art process simulations and techno-economic assessments of ionic liquid-based biogas upgrading techniques: Challenges and prospects. Fuel 2022;314:123064.
[225] Hospital-Benito D, et al. Techno-economic feasibility of ionic liquids-based CO2 chemical capture processes. Chem Eng J 2021;407:127196.
[226] Filburn T, Helble J, Weiss R. Development of supported ethanolamines and modified ethanolamines for CO2 capture. Ind Eng Chem Res 2005;44(5):1542–6.
[227] Ochedi FO, et al. Carbon dioxide capture using liquid absorption methods: a review. Environ Chem Lett 2021;19:77–109.
[228] Gusnawan PJ, et al. Performance and stability of a bio-inspired soybean-based solvent for CO2 capture from flue gas. Chem Eng J 2020;385:123908.
[229] Goff GS, Rochelle GT. Monoethanolamine degradation: O2 mass transfer effects under CO2 capture conditions. Ind Eng Chem Res 2004;43(20):6400–8.

[230] Davis J, Rochelle G. Thermal degradation of monoethanolamine at stripper conditions. Energy Procedia 2009;1(1):327–33.
[231] Ribeiro MS, Zanatta M, Corvo MC. Ionic liquids and biomass as carbon precursors: Synergistically answering a call for CO2 capture and conversion. Fuel 2022;327:125164.
[232] Akinola TE, Oko E, Wang MJF. Study of CO2 removal in natural gas process using mixture of ionic liquid and MEA through process simulation. Fuel 2019;236:135–46.
[233] Kobzar YL, Fatyeyeva K. Ionic liquids as green and sustainable steel corrosion inhibitors: Recent developments. Chem Eng J 2021;425:131480.
[234] Yavuz A, et al. Electrodeposition and Characterisation of Zn-Co Alloys from Ionic Liquids on Copper. J Electron Mater 2022;51(9):5253–61.
[235] Jiang Y, et al. Experimental and theoretical studies on corrosion inhibition behavior of three imidazolium-based ionic liquids for magnesium alloys in sodium chloride solution. J Mol Liq 2022;345:116998.
[236] Scovazzo P, et al. Gas separations using non-hexafluorophosphate [PF6]− anion supported ionic liquid membranes. J Membr Sci 2004;238(1–2):57–63.
[237] Baimoldina A, et al. Separating miscible liquid–liquid mixtures using supported ionic liquid membranes. Ind Eng Chem Res 2021;61(1):747–53.
[238] Goh JTE, et al. Enhanced performance of polymer electrolyte membranes via modification with ionic liquids for fuel cell applications. Membranes 2021;11(6):395.
[239] Yan X, et al. Ionic liquids combined with membrane separation processes: A review. Sep Purif Technol 2019;222:230–53.
[240] Scovazzo P, et al. Long-term, continuous mixed-gas dry fed CO2/CH4 and CO2/N2 separation performance and selectivities for room temperature ionic liquid membranes. J Membr Sci 2009;327(1–2):41–8.
[241] Yoo S, et al. CO2 separation membranes using ionic liquids in a Nafion matrix. J Membr Sci 2010;363(1–2):72–9.
[242] Iarikov D, Hacarlioglu P, Oyama S. Supported room temperature ionic liquid membranes for CO2/CH4 separation. Chem Eng J 2011;166(1):401–6.
[243] Craveiro R, et al. Supported liquid membranes based on deep eutectic solvents for gas separation processes. Sep Purif Technol 2021;254:117593.
[244] Bara JE, et al. Guide to CO2 separations in imidazolium-based room-temperature ionic liquids. Ind Eng Chem Res 2009;48(6):2739–51.
[245] Noble RD, Gin DL. Perspective on ionic liquids and ionic liquid membranes. J Membr Sci 2011;369(1–2):1–4.
[246] Scovazzo P. Determination of the upper limits, benchmarks, and critical properties for gas separations using stabilized room temperature ionic liquid membranes (SILMs) for the purpose of guiding future research. J Membr Sci 2009;343(1–2):199–211.
[247] Robeson LM. The upper bound revisited. J Membr Sci 2008;320(1–2):390–400.
[248] Condemarin R, Scovazzo P. Gas permeabilities, solubilities, diffusivities, and diffusivity correlations for ammonium-based room temperature ionic liquids with comparison to imidazolium and phosphonium RTIL data. Chem Eng J 2009;147(1):51–7.
[249] Scovazzo P. Testing and evaluation of room temperature ionic liquid (RTIL) membranes for gas dehumidification. J Membr Sci 2010;355(1–2):7–17.
[250] Camper D, et al. Bulk-fluid solubility and membrane feasibility of Rmim-based room-temperature ionic liquids. Ind Eng Chem Res 2006;45(18):6279–83.
[251] Bara JE, et al. Gas separations in fluoroalkyl-functionalized room-temperature ionic liquids using supported liquid membranes. Chem Eng J 2009;147(1):43–50.
[252] Neves LA, Crespo JG, Coelhoso IM. Gas permeation studies in supported ionic liquid membranes. J Membr Sci 2010;357(1–2):160–70.
[253] Cserjési P, Nemestóthy N, Bélafi-Bakó K. Gas separation properties of supported liquid membranes prepared with unconventional ionic liquids. J Membr Sci 2010;349(1–2):6–11.
[254] Myers C, et al. High temperature separation of carbon dioxide/hydrogen mixtures using facilitated supported ionic liquid membranes. J Membr Sci 2008;322(1):28–31.
[255] Lozano L, et al. Recent advances in supported ionic liquid membrane technology. J Membr Sci 2011;376(1–2):1–14.
[256] Sang Y, Huang JJ. Benzimidazole-based hyper-cross-linked poly (ionic liquid) s for efficient CO2 capture and conversion. Chem Eng J 2020;385:123973.
[257] Huang Z, et al. Evaluation of supported multi-functionalized amino acid ionic liquid-based sorbents for low temperature CO2 capture. Fuel 2022;310:122284.
[258] Huang Z, et al. Evaluation of supported multi-functionalized amino acid ionic liquid-based sorbents for low temperature CO2 capture. Fuel 2022;310:122284.
[259] Cui C, et al. Ionic-liquid-modified click-based porous organic polymers for controlling capture and catalytic conversion of CO2. ChemSusChem 2020;13(1):180–7.
[260] Ren J, et al. Supported ionic liquid sorbents for CO2 capture from simulated flue-gas. Chin J Chem Eng 2018;26(11):2377–84.
[261] Cao J, et al. Ordered porous poly (ionic liquid) crystallines: spacing confined ionic surface enhancing selective CO2 capture and fixation. ACS Appl Mater Interfaces 2019;11(6):6031–41.
[262] Hernández E, et al. Integrated carbon capture and utilization based on bifunctional ionic liquids to save energy and emissions. Chem Eng J 2022;446:137166.
[263] Sang Y, et al. Bifunctional ionic hyper-cross-linked polymers for CO2 capture and catalytic conversion. Appl Surf Sci 2022;585:152663.
[264] Huang Q, et al. A novel biphasic solvent of amino-functionalized ionic liquid for CO2 capture: High efficiency and regenerability. J CO2 Util 2018;25:22–30.
[265] Zhan X, et al. Dual-functionalized ionic liquid biphasic solvent for carbon dioxide capture: High-efficiency and energy saving. Environ Sci Technol 2020;54(10):6281–8.
[266] Wang Y, et al. A novel process design for CO2 capture and H2S removal from the syngas using ionic liquid. J Cleaner Prod 2019;213:480–90.
[267] Qazi S, et al. CO2 capture in a hollow fiber membrane contactor coupled with ionic liquid: Influence of membrane wetting and process parameters. Separation Purification Technol 2020;233:115986.
[268] Rostami S, Keshavarz P, Raeissi S. Experimental study on the effects of an ionic liquid for CO2 capture using hollow fiber membrane contactors. Int J Greenhouse Gas Control 2018;69:1–7.
[269] Philip FA, Henni AJM, Materials M. Enhancement of post-combustion CO2 capture capacity by incorporation of task-specific ionic liquid into ZIF-8. Microporous Mesoporous Mater 2022;330:111580.
[270] Thomas A, Ahamed R, Prakash MJRA. Selection of a suitable ZIF-8/ionic liquid (IL) based composite for selective CO 2 capture: The role of anions at the interface. RSC Adv 2020;10(64):39160–70.
[271] Mukesh C, et al. Pore size-excluded low viscous porous liquids for CO2 sorption at room temperature and thermodynamic modeling study. J Mol Liq 2022;356:119046.
[272] Yu T, et al. Molecular dynamics studies on separation of CO2/CH4 by the ionic liquids encapsulated ZIF-8. J Membr Sci 2022;644:120117.
[273] Garip M, Gizli N. Ionic liquid containing amine-based silica aerogels for CO2 capture by fixed bed adsorption. J Mol Liquids 2020;310:113227.
[274] Mei M, et al. CO2 capture by 1-ethyl-3-methylimidazolium acetate: Solubility at low pressure and quantification of chemisorption and physisorption. J Mol Liq 2022;348:118036.
[275] de Jesus SS, Maciel Filho R. Are ionic liquids eco-friendly? Renew Sustain Energy Rev 2022;157:112039.
[276] Joglekar HG, Rahman I, Kulkarni BD. The path ahead for ionic liquids. Chem Eng Technol: Ind Chem-Plant Equipment-Process Eng-Biotechnol 2007;30(7):819–28.
[277] Yang Z, et al. Amino acid ionic liquids as anticorrosive and lubricating additives for water and their environmental impact. Tribol Int 2021;153:106663.
[278] Mena I, et al. Cation and anion effect on the biodegradability and toxicity of imidazolium–and choline–based ionic liquids. Chemosphere 2020;240:124947.
[279] Wu S, et al. Assessment of the toxicity and biodegradation of amino acid-based ionic liquids. RSC Adv 2019;9(18):10100–8.
[280] Romero A, et al. Toxicity and biodegradability of imidazolium ionic liquids. J Hazard Mater 2008;151(1):268–73.
[281] Coleman D, Gathergood N. Biodegradation studies of ionic liquids. Chem Soc Rev 2010;39(2):600–37.
[282] Gathergood N, Garcia MT, Scammells PJ. Biodegradable ionic liquids: Part I Concept, preliminary targets and evaluation 2004;6:166–75.
[283] Garcia MT, Gathergood N, Scammells PJ. Biodegradable ionic liquids Part II Effect of the anion and toxicology 2005;7:9–14.
[284] Gathergood N, Scammells PJ, Garcia MT. Biodegradable ionic liquids Part III The first readily biodegradable ionic liquids 2006;8:156–60.
[285] Boethling R, Sommer E, DiFiore D. Designing small molecules for biodegradability. Chem Rev 2007;107(6):2207–27.
[286] Buettner CS, et al. Surface-active ionic liquids: A review. J Mol Liq 2022;347:118160.
[287] Verma S, et al. Drastic influence of amide functionality and alkyl chain length dependent physical, thermal and structural properties of new pyridinium-amide cation based biodegradable room temperature ionic liquids. J Mol Struct 2022;1250:131679.
[288] Morrissey S, et al. Biodegradable, non-bactericidal oxygen-functionalised imidazolium esters: A step towards 'greener'ionic liquids. Green Chem 2009;11(4):475–83.
[289] Harjani JR, et al. Biodegradable pyridinium ionic liquids: design, synthesis and evaluation. Green Chem 2009;11(1):83–90.
[290] Zhang C, et al. Biodegradation of pyridinium-based ionic liquids by an axenic culture of soil Corynebacteria. Green Chem 2010;12(5):851–8.
[291] Ford L, et al. Further studies on the biodegradation of ionic liquids. Green Chem 2010;12(10):1783–9.
[292] Kowalska D, et al. Ionic liquids as environmental hazards–Crucial data in view of future PBT and PMT assessment. J Hazard Mater 2021;403:123896.
[293] Zhao D, Liao Y, Zhang Z. Toxicity of ionic liquids. Clean–soil, air, water 2007;35(1):42–8.
[294] Petkovic M, et al. Ionic liquids: a pathway to environmental acceptability. Chem Soc Rev 2011;40(3):1383–403.
[295] Flieger J, Flieger M. Ionic liquids toxicity—benefits and threats. Int J Mol Sci 2020;21(17):6267.
[296] Gonçalves AR, et al. Ionic liquids—A review of their toxicity to living organisms. Int J Mol Sci 2021;22(11):5612.
[297] Yan F, et al. Norm index-based QSTR model to predict the eco-toxicity of ionic liquids towards Leukemia rat cell line. Chemosphere 2019;234:116–22.
[298] Cho C-W, et al. Review of the toxic effects of ionic liquids. Sci Total Environ 2021;786:147309.
[299] Matzke M, et al. The influence of anion species on the toxicity of 1-alkyl-3-methylimidazolium ionic liquids observed in an (eco) toxicological test battery. Green Chem 2007;9(11):1198–207.
[300] Couling DJ, et al. Assessing the factors responsible for ionic liquid toxicity to aquatic organisms via quantitative structure–property relationship modeling. Green Chem 2006;8(1):82–90.
[301] Wells AS, Coombe VT. On the freshwater ecotoxicity and biodegradation properties of some common ionic liquids. Org Process Res Dev 2006;10(4):794–8.
[302] Hernández-Fernández F, et al. Exploring ionic liquids based on pyrrolidinium and imidazolium cations with low toxicity towards Escherichia coli for designing sustainable bioprocesses. J Biotechnol 2022;360:192–7.

[303] Baruah P, et al. Therapeutic opportunities of surface-active ionic liquids: a case study on acetylcholinesterase, citrate synthase and HeLa cell lines. New J Chem 2022;46(42):20419–32.
[304] Fütyű J, et al. Recyclable supported Brønsted acidic ionic liquid catalysts with non-aromatic cations for the oligomerization of isobutene under mild conditions. Mol Catal 2022;518:112075.
[305] Sani ASA, et al. Machining performance of vegetable oil with phosphonium-and ammonium-based ionic liquids via MQL technique. J Clean Prod 2019;209:947–64.
[306] Ghanem OB, et al. Greener approach for the separation of naphthenic acid from model oil using Pyrrolidinium-based amino acid ionic liquids. Fuel 2023;337:127141.
[307] Stolte S, et al. Effects of different head groups and functionalised side chains on the aquatic toxicity of ionic liquids. Green Chem 2007;9(11):1170–9.
[308] Padilla MS, et al. Expanding the structural diversity of hydrophobic ionic liquids: Physicochemical properties and toxicity of Gemini ionic liquids. Green Chem 2021;23(12):4375–85.
[309] Pretti C, et al. Acute toxicity of ionic liquids for three freshwater organisms: Pseudokirchneriella subcapitata, Daphnia magna and Danio rerio. Ecotoxicol Environ Saf 2009;72(4):1170–6.
[310] Frade RF, Afonso CA. Impact of ionic liquids in environment and humans: an overview. Hum Exp Toxicol 2010;29(12):1038–54.
[311] Vieira NS, et al. Acute aquatic toxicity and biodegradability of fluorinated ionic liquids. ACS Sustain Chem Eng 2019;7(4):3733–41.
[312] Cłapa T, et al. Morpholinium-based ionic liquids show antimicrobial activity against clinical isolates of Pseudomonas aeruginosa. Res Microbiol 2021;172(3):103817.
[313] Muhammad Shahbaz, Suzana Yusup, Abrar Inayat, Muhammad Ammar, David Onoja Patrick, Angga Pratama, and Salman Raza Naqvi. Syngas Production from Steam Gasification of Palm Kernel Shell with Subsequent CO_2 Capture Using CaO Sorbent: An Aspen Plus Modeling. Energy & Fuels 2017 31 (11), 12350-12357.
[314] Azeem Sarwar, Majid Ali, Asif Hussain Khoja, Azra Nawar, Adeel Waqas, Rabia Liaquat, Salman Raza Naqvi, Muhammad Asjid, Synthesis and characterization of biomass-derived surface-modified activated carbon for enhanced CO2 adsorption, Journal of CO2 Utilization, Volume 46, 2021, 101476, ISSN 2212-9820, https://doi.org/10.1016/j.jcou.2021.101476.